

Electronic Supplementary Information

Self-regulated catalysis for selective synthesis of primary amines from carbonyl compounds

*Mingxia Gao,^{a,b} Xiuquan Jia,^a Jiping Ma,^{*a} Xiaomeng Fan,^{a,b} Jin Gao^a and Jie Xu^{*a}*

^aState Key Laboratory of Catalysis, Dalian National Laboratory for Clean Energy, Dalian Institute of Chemical Physics, Chinese Academy of Sciences, Dalian 116023, P. R. China.

^bUniversity of Chinese Academy of Sciences, Beijing 100049, P. R. China.

Table of Contents

1. Materials	3
2. Supplementary Equations	7
3. Derivation of Reaction Rate Laws	8
4. Additional Results.....	10
5. GC, MS and NMR Spectra	19
6. Standard Curves	49
References.....	50

1. Materials

All chemicals and reagents are of analytical grade and used as purchased without further purification. Following are the detail list of the used chemicals and reagents.

Table S1. The detail list of the used chemicals and reagents.

Chemicals	Purity	Corporation
RuCl ₃ ·H ₂ O	40-42% metal basis	Tianjin Jinbolan Fine Chemical Co., Ltd, China
LDHs	98%	Tianjin Heowns Biochem LLC (China)
h-BN	99.9%	Shanghai Aladdin Biochemical Technology Co., Ltd. China
Activated carbon	>100 mesh	
γ-Al ₂ O ₃	99.9% metals basis, 10 nm	
TiO ₂	99.99% metals basis	
MgO	AR	
SiO ₂	99.99% metals basis	
Cobalt(II) nitrate hexahydrate	AR	
Palladium chloride	59-60% metal basis	
Rhodium (III) Chloride Hydrate	38.5-42.5%	
Sodium borohydride	98%	
Furfuryl alcohol	AR	
1,3,5-Trimethylbenzene	AR	
Benzaldehyde	99%	
p-Anisaldehyde	99%	
4-Chlorobenzaldehyde	98%	
4-Bromobenzaldehyde	99%	
3-Methoxybenzylamine	98%	
4-Methoxybenzylamine	98%	
4-Fluorobenzylamine	99%	
4-Methylbenzylamine	98%	
3-Methylbenzylamine	97%	
Phenylpropyl aldehyde	95%	
3-Phenyl-1-propylamine	98%	
Cyclopentylamine	99%	
NH ₃ ·H ₂ O	25-28 wt%	Tianjin Kemiou Chemical Reagent Co., Ltd, China
HCl	AR	
Cyclohexanone	AR	
Cupric nitrate	AR	
Furfural	AR	Sinopharm Chemical Reagent

L-Lysine	BR	Co., Ltd. China
Methanol	AR	
Cyclopentanone	CP	
2-Hydroxybenzaldehyde	CP	
Furfurylamine	AR	Shanghai McLean Biochemical Technology Co., Ltd. China
Tetrahydrofurfurylamine	AR	
p-Tolualdehyde	99%	
m-Tolualdehyde	99%	
2-Methylbenzaldehyde	98%	
5-Methyl furfural	97%	Tokyo Chemical Industry Co., Ltd.
3-Methoxybenzaldehyde	98%	
5-Methylfurfurylamine	98%	
Cyclohexylamine	99%	
Bis(2-furylmethyl)amine	95%	Enamine Ltd., Ukraine
5-Hydroxymethylfurfural	98%	Innochem (Beijing) Technology Co., Ltd.
Benzofuran-2-carboxaldehyde	99%	Alfa Aesar (China) Chemicals Co., Ltd.
4-Chlorobenzylamine	98%	Saan Chemical Technology (Shanghai) Co., Ltd.
4-Bromobenzylamine	97%	
3-Hydroxybenzylamine	97%	
4-Fluorobenzaldehyde	98%	Shanghai Yuanye Biological Technology Co., Ltd.
2-Hydroxybenzylamine	95%	
3-Hydroxybenzaldehyde	98%	
2-Methylbenzylamine	99%	Shanghai Bide Pharmatech Co., Ltd.
Benzylamine	99%	Sigma-Aldrich (Shanghai) Trading Co., Ltd.

Procedure for synthesis of N-furfurylidenefurfurylamine (4a)

The **4a** was synthesized via the condensation of furfural and furfurylamine in a round bottom flask within an oil bath. 2.0 mmol furfural, 2.0 mmol furfurylamine and 7.0 mL MeOH were loaded into the flask. Then it was heated to 30 °C with stirring for 2 hours. After the reaction was completed, the solvent was removed by rotary evaporation under vacuum, and the extraction was repeated 5 times with ethyl acetate and water (2:1). The upper ethyl acetate solution was collected, and dried with anhydrous sodium sulfate. The

resulting filtrate was rotary evaporated under vacuum to remove the solvent to obtain the **4a** as yellow-brown liquid in 98% yield by GC (**Figure S36** in the supplementary materials).

Procedure for isolation and identification of products

Furfurylamine (3a): After the reaction was completed, the catalyst was separated by filtration and the obtained solution was then separated using thin layer chromatography (eluent: ethyl acetate / ethyl alcohol = 100:1, v/v). The filtrate was evaporated to obtain the pure **3a** (95% yield). ¹H NMR (400 MHz, DMSO-D₆, 298 K): δ = 7.51 (s, 1H, Ar), 6.35 (dd, J = 2.9, 1.9 Hz, 1H, Ar), 6.21-6.15 (m, 1H, Ar), 3.65 (s, 2H, CH₂), 1.70 (brs, 2H, NH₂), ¹³C NMR (100 MHz, DMSO-D₆, 298 K): δ = 157.59, 141.24, 110.19, 104.72, 38.74.

4-Methoxybenzylamine (3f): After the reaction was completed, the catalyst was separated by filtration and the obtained solution was then separated using thin layer chromatography (eluent: ethyl acetate / ethyl alcohol = 100:1, v/v). The filtrate was evaporated to obtain the pure **3f** (91% yield). ¹H NMR (400 MHz, DMSO-D₆, 298 K): δ = 7.23 (d, J = 8.3 Hz, 2H, Ar), 6.85 (d, J = 8.5 Hz, 2H, Ar), 3.72 (s, 3H, CH₃), 3.63 (s, 2H, CH₂), 1.66 (brs, 2H, NH₂), ¹³C NMR (100 MHz, DMSO-D₆, 298 K): δ = 157.72, 136.32, 128.05, 113.42, 54.96, 45.05.

4-Fluorobenzylamine (3h): After the reaction was completed, the catalyst was separated by filtration and the obtained solution was then separated using thin layer chromatography (eluent: ethyl acetate / ethyl alcohol = 10:1, v/v). The filtrate was evaporated to obtain the pure **3h** (90% yield). ¹H NMR (400 MHz, DMSO-D₆, 298 K): δ = 7.35 (dd, J = 8.3, 5.9 Hz, 2H, Ar), 7.10 (dd, J = 14.7, 5.9 Hz, 2H, Ar), 3.69 (s, 2H, CH₂), 1.77 (brs, 2H, NH₂), ¹³C NMR (100 MHz, DMSO-D₆, 298 K): δ = 161.99, 159.60, 140.43, 128.72, 114.71, 114.50, 44.85.

4-Methylbenzylamine (3k): After the reaction was completed, the catalyst was separated by filtration and the obtained solution was then separated using thin layer chromatography (eluent: ethyl acetate). The filtrate was evaporated to obtain the pure **3k** (96% yield). ¹H NMR (400 MHz, DMSO-D₆, 298 K): δ = 7.20 (d, J = 7.8 Hz, 2H, Ar), 7.09 (d, J = 7.8 Hz, 2H, Ar), 3.65 (s, 2H, CH₂), 2.26 (s, 3H, CH₃), 1.67 (brs, 2H, NH₂), ¹³C NMR (100 MHz, DMSO-D₆, 298 K): δ = 141.25, 134.94, 128.57, 126.88, 45.38, 20.62.

Cyclohexylamine (3o): After the reaction was completed, the catalyst was separated by filtration and the obtained solution was then separated using thin layer chromatography (eluent: ethyl acetate / ethyl alcohol = 2:1, v/v). The filtrate was evaporated to obtain the pure **3o** (89% yield). ¹H NMR (400 MHz, DMSO-D₆, 298 K): δ = 2.48 (tt, J = 10.3, 3.7 Hz, 1H), 1.71 (d, J = 2.7 Hz, 1H), 1.69-1.62 (m, 2H), 1.69-1.34 (m, 4H), 1.34-0.87 (m, 6H), ¹³C NMR (100 MHz, DMSO-D₆, 298 K): δ = 49.97, 36.44, 25.47, 24.64.

3-Hydroxybenzylamine (3r): After the reaction was completed, the catalyst was separated by filtration and the obtained solution was evaporated and dried in vacuo to give the pure **3r** (91% yield). ¹H NMR (400 MHz, DMSO-D₆, 298 K): δ = 7.07 (t, J = 7.7 Hz, 1H, Ar), 6.74 (s, 1H, Ar), 6.71 (d, J = 7.5 Hz, 1H, Ar), 6.59 (d, J = 7.9 Hz, 1H, Ar), 3.62 (s, 2H, CH₂), ¹³C NMR (100 MHz, DMSO-D₆, 298 K): δ = 157.38, 145.58, 128.96, 117.52, 113.94, 113.14, 45.58.

2. Supplementary Equations

The conversion of substrate (mol%), yield (mol%) of products and the TOF (min^{-1}) of the reaction were calculated according to the following formula:

$$\text{Conversion (\%)} = \left(1 - \frac{\text{Moles of substrate after reaction}}{\text{Moles of substrate loaded initially}} \right) \times 100\% \quad (\text{S1})$$

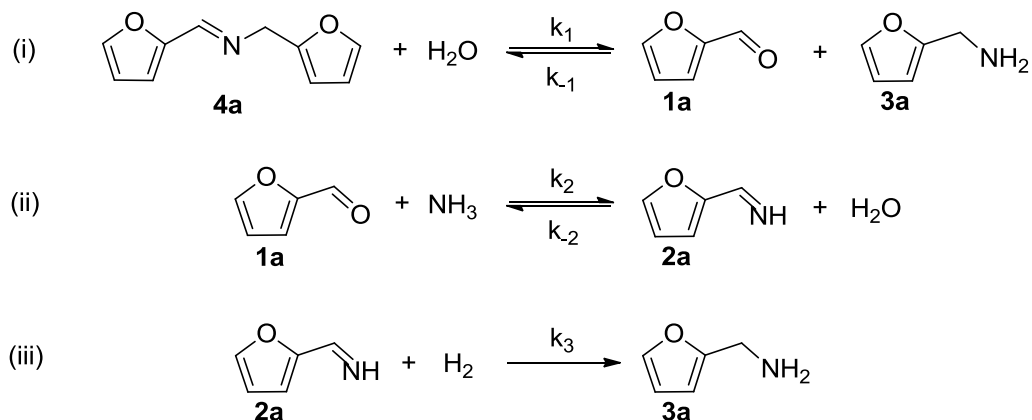
Yield (%) =

$$\left(\frac{\text{Moles of product after reaction} \times \text{Number of Carbon in product}}{\text{Moles of substrate loaded initially} \times \text{Number of Carbon in substrate}} \right) \times 100\% \quad (\text{S2})$$

$$\text{TOF (\text{min}^{-1})} = \frac{\text{Moles of } \mathbf{3a} \text{ formed via hydrogenation}}{\text{Moles of catalyst metal content} \times \text{Reaction time}} \quad (\text{S3})$$

$$\text{NH}_3 \text{ utilization efficiency (\%)} = \frac{\text{Yield of } \mathbf{3} \times \text{Moles of substrate loaded initially}}{\text{Moles of NH}_3 \text{ loaded initially}} \quad (\text{S4})$$

3. Derivation of Reaction Rate Laws



Scheme S1. Stepwise description for the hydrogenolysis of the imine of **4a**.

The hydrogenolysis of the imine of **4a** is presented in Scheme S1.

Full rate law derivation:

$$\frac{d[\mathbf{1a}]}{dt} = k_1[\mathbf{4a}][\text{H}_2\text{O}] - k_{-1}[\mathbf{1a}][\mathbf{3a}] - k_2[\mathbf{1a}][\text{NH}_3] + k_{-2}[\mathbf{2a}][\text{H}_2\text{O}] \quad (\text{S5})$$

$$\frac{d[\mathbf{2a}]}{dt} = k_2[\mathbf{1a}][\text{NH}_3] - k_{-2}[\mathbf{2a}][\text{H}_2\text{O}] - k_3[\mathbf{2a}][\text{H}_2] \quad (\text{S6})$$

$$\text{rate} = \frac{d[\mathbf{3a}]}{dt} = k_3[\mathbf{2a}][\text{H}_2] + k_1[\mathbf{4a}][\text{H}_2\text{O}] - k_{-1}[\mathbf{1a}][\mathbf{3a}] \quad (\text{S7})$$

Apply steady-state approximation to **1a** and **2a**, then:

$$\frac{d[\mathbf{1a}]}{dt} = 0 \quad (\text{S8}) \quad k_1[\mathbf{4a}][\text{H}_2\text{O}] - k_{-1}[\mathbf{1a}][\mathbf{3a}] = k_2[\mathbf{1a}][\text{NH}_3] - k_{-2}[\mathbf{2a}][\text{H}_2\text{O}] \quad (\text{S9})$$

$$\frac{d[\mathbf{2a}]}{dt} = 0 \quad (\text{S10}) \quad k_3[\mathbf{2a}][\text{H}_2] = k_2[\mathbf{1a}][\text{NH}_3] - k_{-2}[\mathbf{2a}][\text{H}_2\text{O}] \quad (\text{S11})$$

If the (i) hydrolysis of **4a** is rate-limiting step, the reaction rate law is deduced as follows:

$$\text{rate} = \frac{d[\mathbf{3a}]}{dt} = 2(k_1[\mathbf{4a}][\text{H}_2\text{O}] - k_{-1}[\mathbf{1a}][\mathbf{3a}]) \quad (\text{S12})$$

As a result of the (ii) rapid amination of **1a** and subsequent (iii) hydrogenation of **2a** to **3a**, [**1a**] should be kept to a minimum, thus:

$$\text{rate} = \frac{d[\mathbf{3a}]}{dt} = 2k_1[\mathbf{4a}][\text{H}_2\text{O}] \quad (\text{S13})$$

If the (iii) hydrogenation of primary aldimine is the rate-limiting step, the reaction rate law is deduced as follows.

Apply equilibrium hypothesis to **1a**, then:

$$\frac{d[\mathbf{1a}]}{dt} = k_1[\mathbf{4a}][\text{H}_2\text{O}] - k_{-1}[\mathbf{1a}][\mathbf{3a}] = 0 \quad (\text{S14})$$

$$[\mathbf{1a}] = \frac{k_1[\mathbf{4a}][\text{H}_2\text{O}]}{k_{-1}[\mathbf{3a}]} \quad (\text{S15})$$

Apply equilibrium hypothesis to **2a**, then:

$$\frac{d[\mathbf{2a}]}{dt} = k_2[\mathbf{1a}][\text{NH}_3] - k_{-2}[\mathbf{2a}][\text{H}_2\text{O}] = 0 \quad (\text{S16})$$

$$[\mathbf{2a}] = \frac{k_2[\mathbf{1a}][\text{NH}_3]}{k_{-2}[\text{H}_2\text{O}]} \quad (\text{S17})$$

Substituting equation S15 and equation S17 into equation S7, then:

$$\text{rate} = \frac{d[\mathbf{3a}]}{dt} = 2k_3[\mathbf{2a}][\text{H}_2\text{O}] = \frac{2k_1k_2k_3[\mathbf{4a}][\text{NH}_3][\text{H}_2\text{O}]}{k_{-1}k_{-2}[\mathbf{3a}]} \quad (\text{S18})$$

4. Additional Results

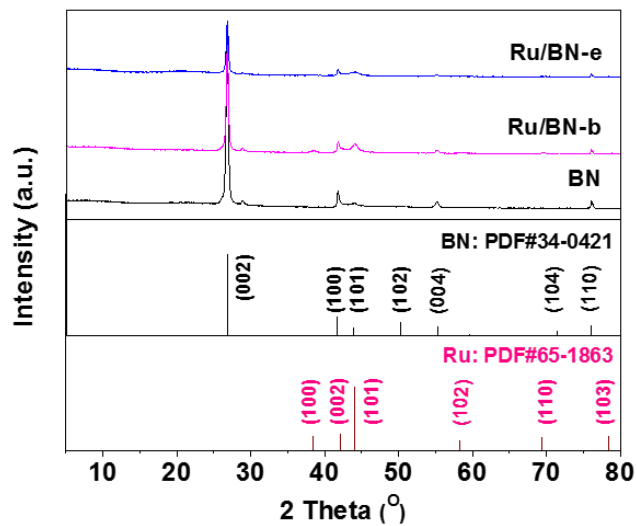


Figure S1. XRD of Ru/BN-e and Ru/BN-b.

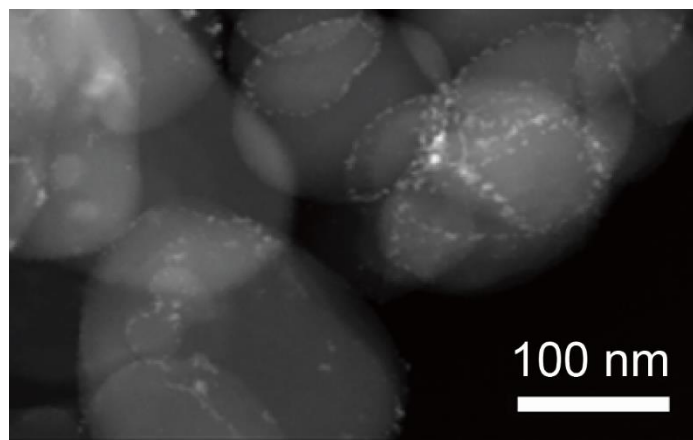


Figure S2. STEM image of Ru/BN-e.

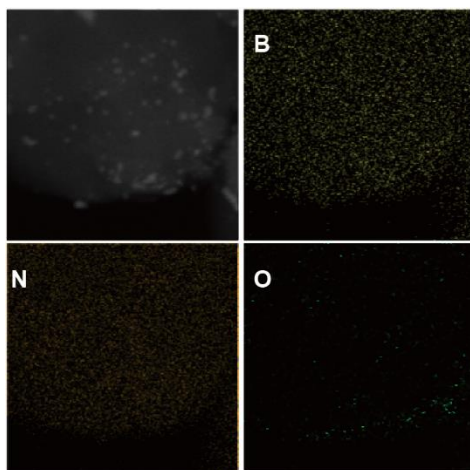


Figure S3. STEM-EDS element mapping of Ru/BN-b catalyst.

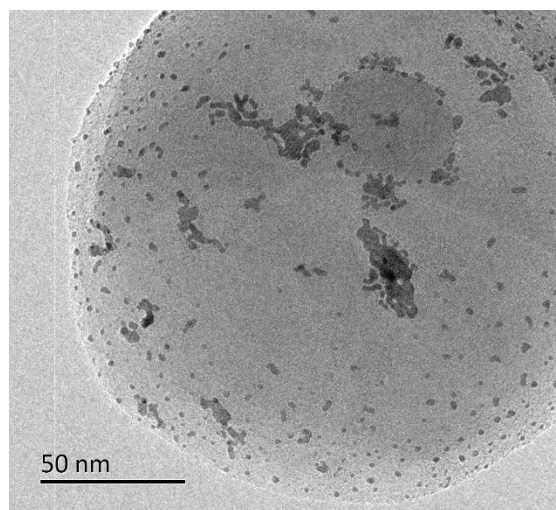


Figure S4. TEM image of Ru/BN with preferential dispersion of Ru on the boundary of the basal plane.

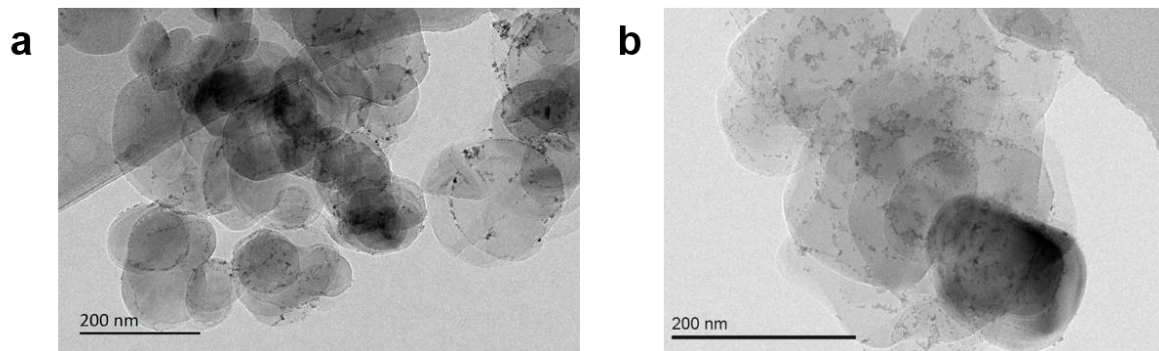


Figure S5. TEM images and particle size distributions of Ru/BN-e (a) and Ru/BN-b (b).

Table S2. ICP-OES and specific surface area results of Ru/BN-e and Ru/BN-b.

Catalyst	Ru Content (wt%)	S_{BET} (m² g⁻¹)
Ru/BN-e	4.2	28.8
Ru/BN-b	4.0	26.6

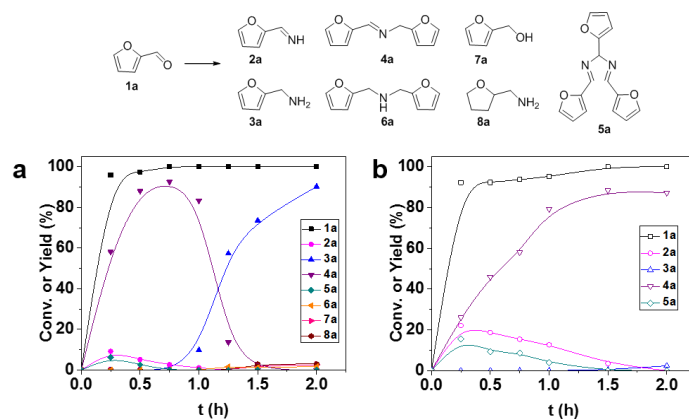


Figure S6. Time courses of the reductive amination of **1a** over (a) Ru/BN-e and (b) Ru/BN-b, respectively. Reaction conditions: 2.0 mmol **1a**, 2 equivalents (equiv) 25% aqueous ammonia, 30 mg catalyst, 7.0 mL MeOH, 1.5 MPa H₂, 90 °C.

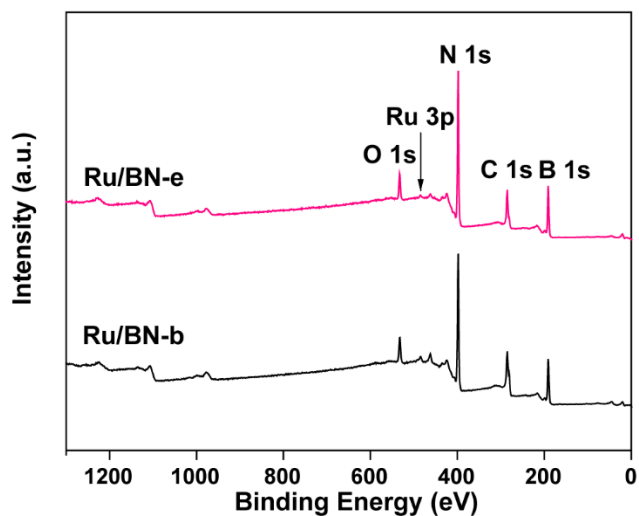


Figure S7. XPS survey spectra of Ru/BN-e versus Ru/BN-b catalysts.

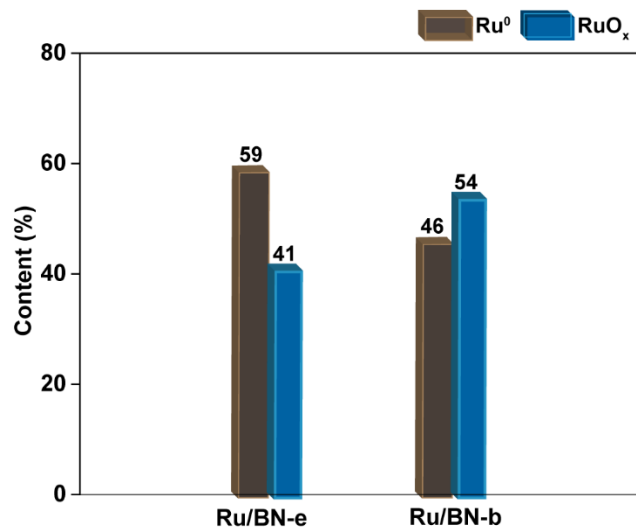


Figure S8. The Ru⁰ and RuO_x contents of the Ru/BN-e versus Ru/BN-b catalysts

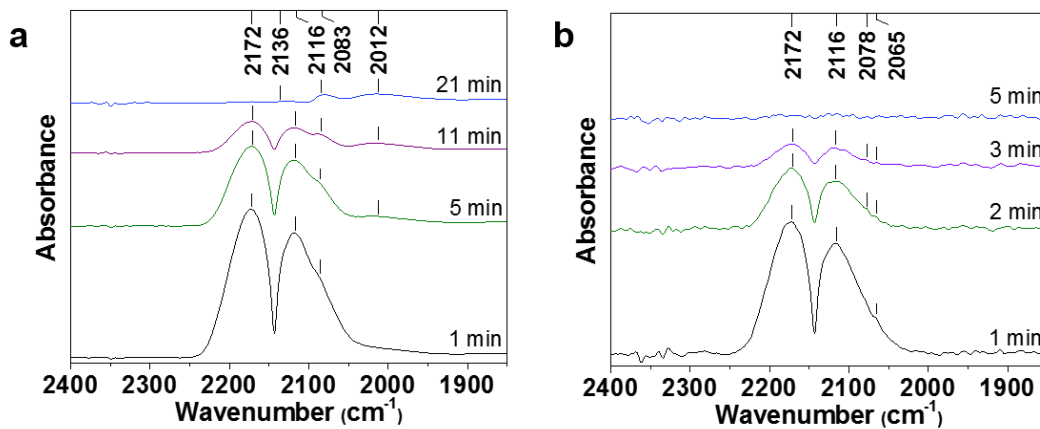
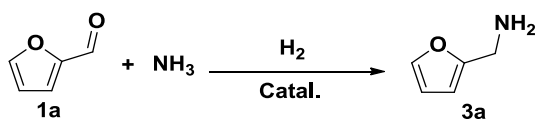


Figure S9. CO-FTIR profiles of (a) Ru/BN-e and (b) Ru/BN-b.

Table S3. Reported catalytic systems for reductive amination of furfural (**1a**) with NH₃ and H₂.

Ref.	Catal.	Catalyst Description	Substrate (mmol)	Solvent	NH ₃ (mmol)	pH ₂ (MPa)	Temp. (°C)	Time (h)	Yield of 3a (%)
1	Ru/Nb ₂ O ₅	Ru supported on Nb ₂ O ₅	0.5	MeOH	8	4.0	90	4	89
2	Ru/Nb ₂ O ₅ ·nH ₂ O-300	Ru supported on niobic acid reduced at 300 °C	0.5	MeOH	8	4.0	70	4	89
3	Ru/Nb ₂ O ₅ -L	Ru supported on layered niobium oxide	2	MeOH	10	2.0	90	8	60
4	Ru-NP	Ru nanoparticles	0.5	MeOH	8	2.0	90	2	99
5	Ru/HAP	Ru supported on hydroxyapatite	1	H ₂ O	44	0.4	100	2	60
6	Rh/Al ₂ O ₃	Rh supported on Al ₂ O ₃	2.1	H ₂ O	69	2	80	2	91.5
7	Co@NC-800	Co nanoparticles supported on nitrogen-doped carbon materials prepared by pyrolysis at 800 °C	1	EtOH	28	1.0	130	12	81.8
8	Ni ₆ AlO _x	Nickel-aluminium oxide	1	H ₂ O	49	0.4	100	5	90
9 ^a	Ni/SiO ₂	Ni supported on SiO ₂	4	40:1 Dioxane :Water (wt.)	20	5.2	130	10	94
10	Ni/NiO@C-700-200-2h-EtOH	Thin graphene spheres encapsulated Ni/NiO nanoalloy catalysts, Ni(NO ₃) ₂ ·6H ₂ O were dissolved in ethanol, pyrolysis temperature 700 °C and 200 °C oxidation for 2 h	0.5	MeOH	10	2.0	90	4	53
This work ^b	Ru/BN-e	Ru on the edge surface of h-BN	2	MeOH	4	1.0	90	5	>99

^a1.0 equiv **3a** was added before reaction to form secondary imine, as the secondary imine exhibited significantly improved resistance to homogeneous reactions with ammonia over Ni/SiO₂. ^b1.1 equiv **3a** was added before reaction to investigate the primary amine effect on the reaction kinetic over Ru/BN-e.

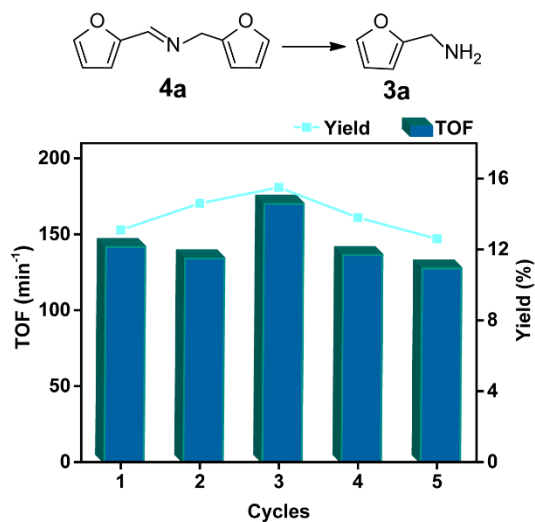


Figure S10. Recyclability test results for the hydrogenolysis of N-furfurylidene-furfurylamine (**4a**) over Ru/BN-e. Reaction conditions: 2.0 mmol **4a**, 1.2 equiv 25% aqueous ammonia, 15 mg catalyst, 7.0 mL MeOH, 1.5 MPa H₂, 90 °C, 15 min.

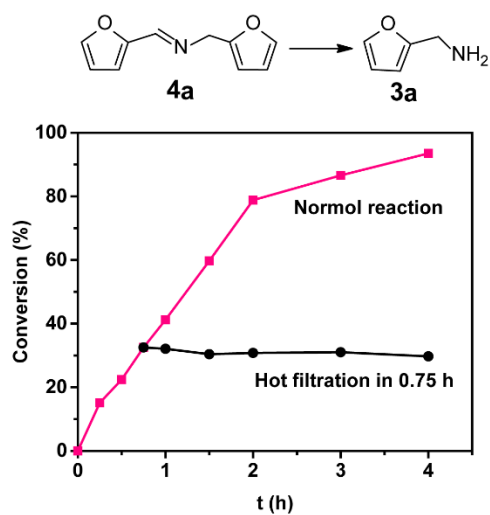
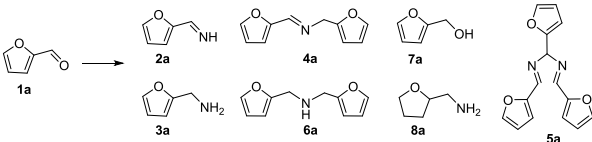


Figure S11. Filtration test by Ru/BN-e. Reaction conditions: 2.0 mmol **4a**, 1.2 equiv 25% aqueous ammonia, 15 mg catalyst, 7.0 mL MeOH, 1.5 MPa H₂, 90 °C. The catalyst was filtrated at 0.75 h.

Table S4. Catalytic conversion of furfural (**1a**) over different catalysts.^a

Entry	Catalyst	Conv. (%)	Yield (%)					
			3a	4a	5a	6a	7a	8a
1	Ru/C	>99	34.3	-	-	4.6	5.7	1.1
2	Ru/TiO ₂	>99	33.1	-	-	-	-	7.4
3	Ru/Al ₂ O ₃	>99	53.5	-	-	-	-	-
4	Ru/SiO ₂	>99	74.2	-	-	3.8	8.8	14.4
5	Ru/MgO	>99	52.8	-	-	-	-	-
6	Ru/LDHs	>99	62.4	-	-	-	-	-
7	Ru/BN-e	>99	90.2	-	-	1.7	2.6	3
8 ^b	Ru/BN-e	>99	92.7	-	-	1.0	2.3	2.4
9 ^c	Ru/BN-e	>99	95.9	-	-	-	2.2	1.7
10	Ru/BN-b	>99	2.4	87.2	-	-	-	-
11 ^b	Ru/BN-b	>99	10.6	64.9	-	-	-	-
12 ^c	Ru/BN-b	>99	22.9	59.3	-	1.5	-	-
13 ^d	Pd/BN	>99	-	-	-	62.4	-	-
14	Rh/BN	>99	17.2	16.6	-	20.8	-	-
15 ^e	Co/BN	73.1	-	-	9.9	-	-	-
16 ^e	Cu/BN	85.2	-	-	4.2	-	-	-

^aReaction conditions: 2.0 mmol **1a**, 2 equiv 25% aqueous ammonia, 30 mg catalyst (metal content: 0.6 mol%), 7.0 mL MeOH, 1.5 MPa H₂, 90 °C, 2 h. ^b3 equiv 25% aqueous ammonia. ^c4 equiv 25% aqueous ammonia. ^dN-[(tetrahydro-2-furyl)methyl] was detected. ^e2,4,5-tris(2-furyl)imidazoline was detected.

The Ru/C and Ru/TiO₂ catalysts (entries 1 and 2) showed low yields of **3a** (33.1% and 34.3%). In the case of Al₂O₃, SiO₂, MgO and LDHs supported Ru catalysts, medium to good yields of **3a** (52.8-74.2%) were observed (entries 3-6). Enhanced and tunable selectivity in reductive amination reaction was exclusively observed over the Ru/BN catalysts (entries 7-12). In the case of Pd and Rh supported on h-BN, 62.4% and 20.8% yields of secondary amine of **6a** were detected, respectively (entries 13 and 14). Co/BN and Cu/BN provided the oligomers of 2,4,5-tris(2-

furyl)imidazoline as the main products, without the occurrence of the reductive amination reaction (entries 15 and 16).

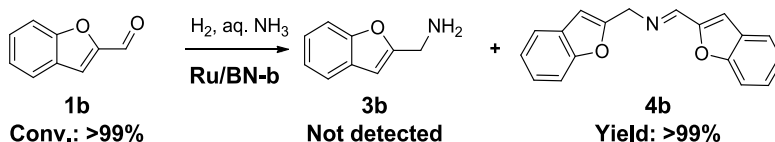


Figure S12. Catalytic reductive amination reaction of benzofuran-2-carboxaldehyde (**1b**). Reaction conditions: 2.0 mmol **1b**, 2 equiv 25% aqueous ammonia, 30 mg Ru/BN-b (0.6 mol%), 7.0 mL MeOH, 1.5 MPa H₂, 90 °C, 2 h.

Benzofuran derivatives as a major group in nature's collection of biologically active heterocycles, have drawn considerable attention due to their profound physiological and chemotherapeutic properties. Herein, the corresponding derivatives of imine and primary amine could be synthesized in enhanced selectivity from benzofuran-2-carboxaldehyde over Ru/BN-b and Ru/BN-e, respectively (**Figure 7** in the main text and **Figure S35, S59** in the supplementary materials).

5. GC, MS and NMR Spectra

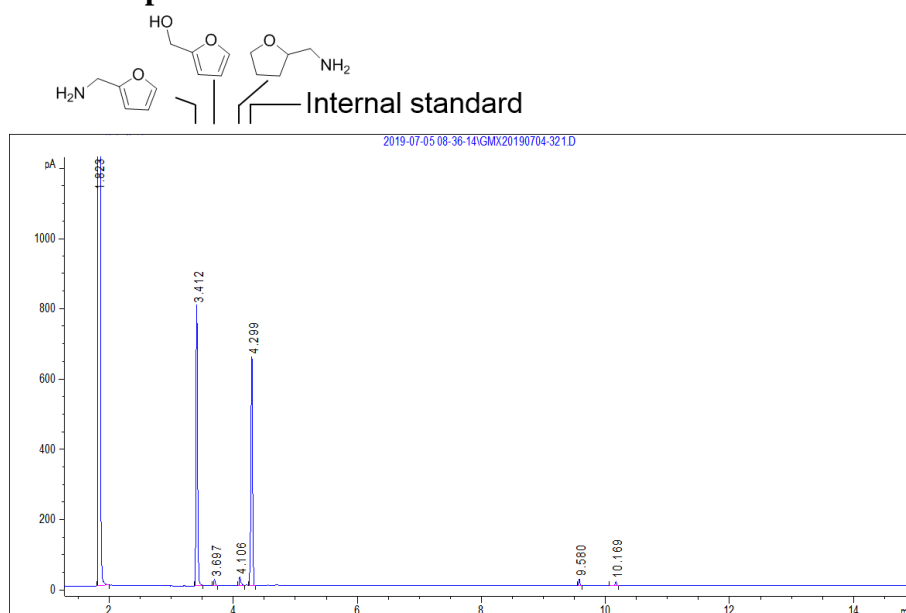


Figure S13. GC spectrum of the typical reaction mixture (**Figure 3** in the main text). Reaction conditions: 2.0 mmol **1a**, 2 equiv 25% aqueous ammonia, 30 mg Ru/BN-e (0.6 mol%), 7.0 mL MeOH, 1.5 MPa H₂, 90 °C, 2 h.

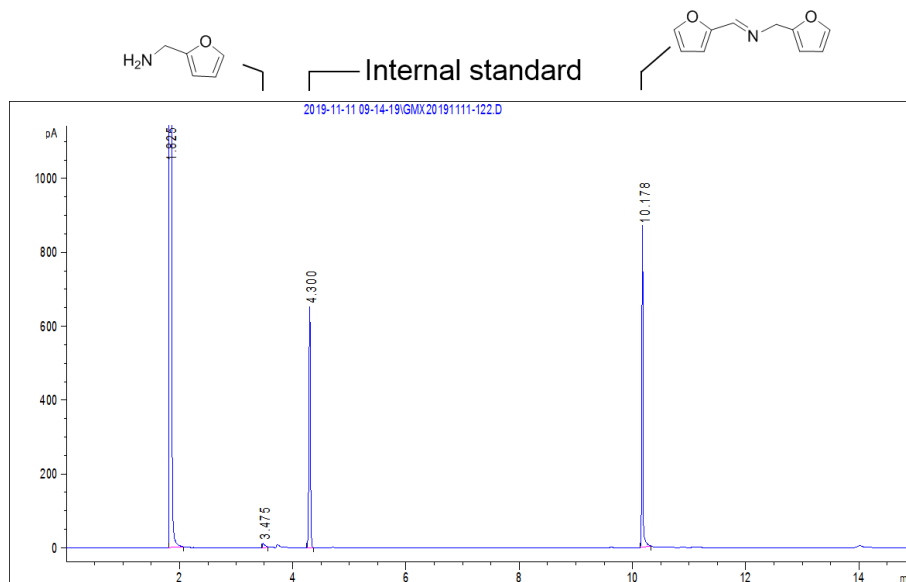


Figure S14. GC spectrum of the reaction mixture (**Figure 3** in the main text). Reaction conditions: 2.0 mmol **1a**, 2 equiv 25% aqueous ammonia, 30 mg Ru/BN-b (0.6 mol%), 7.0 mL MeOH, 1.5 MPa H₂, 90 °C, 2 h.

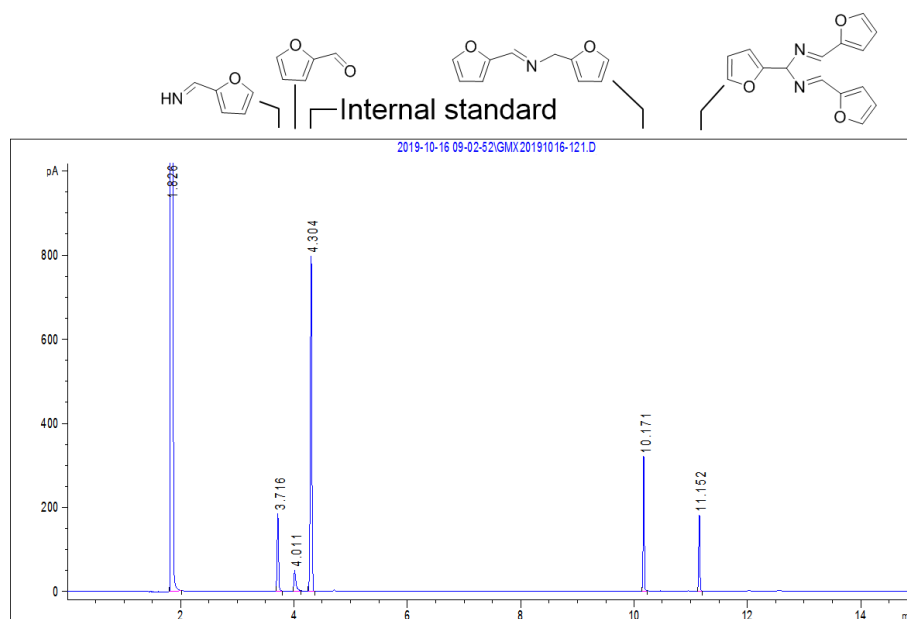


Figure S15. GC spectrum of the reaction mixture (**Figure S6** in the supplementary materials). Reaction conditions: 2.0 mmol **1a**, 2 equiv 25% aqueous ammonia, 30 mg Ru/BN-b (0.6 mol%), 7.0 mL MeOH, 1.5 MPa H₂, 90 °C, 15 min.

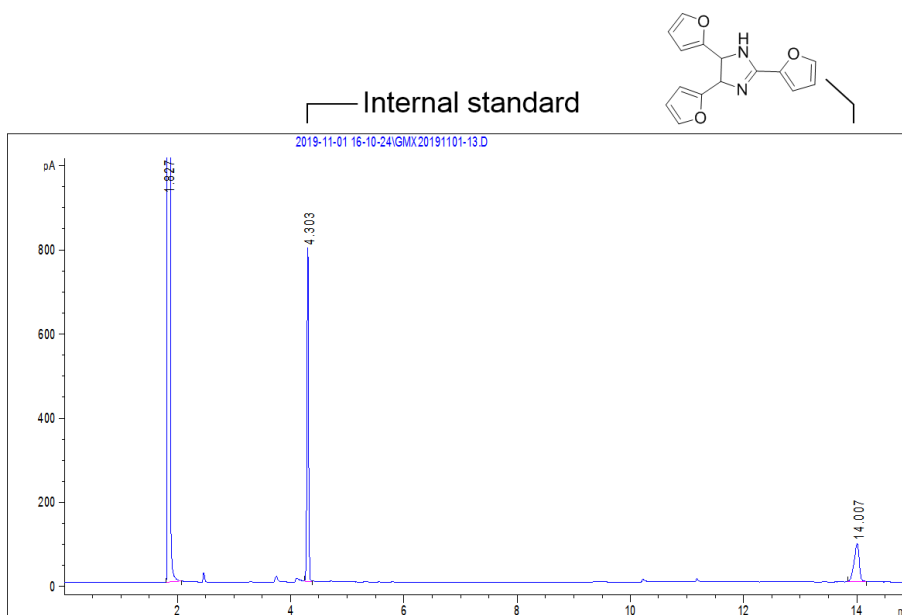


Figure S16. GC spectrum of the reaction mixture for synthesis of 2,4,5-tris(2-furyl)imidazoline. Reaction conditions: 2.0 mmol **1a**, 7 equiv 25% aqueous ammonia, 7.0 mL MeOH, 2.0 MPa H₂, 90 °C, 4 h. The 2,4,5-tris(2-furyl)imidazoline was synthesized according to the reported work,¹ which showed different retention time compared with **5a** (**Figure S15** in the supplementary materials).

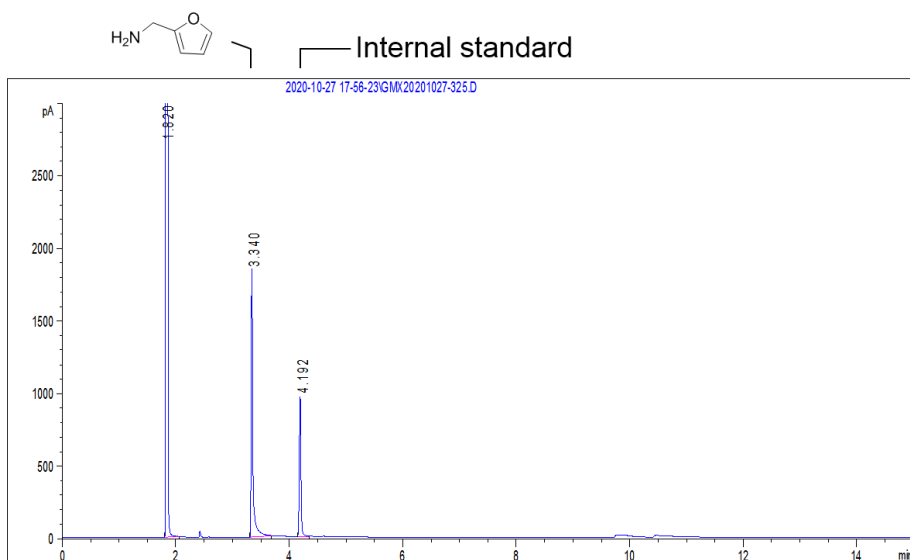


Figure S17. GC spectrum of the reaction mixture (**Figure 7** in the main text). Reaction conditions: 2.0 mmol **1a**, 2.2 mmol **3a**, 2 equiv 25% aqueous ammonia, 30 mg Ru/BN-e (0.6 mol%), 7.0 mL MeOH, 1.0 MPa H₂, 90 °C, 5 h.

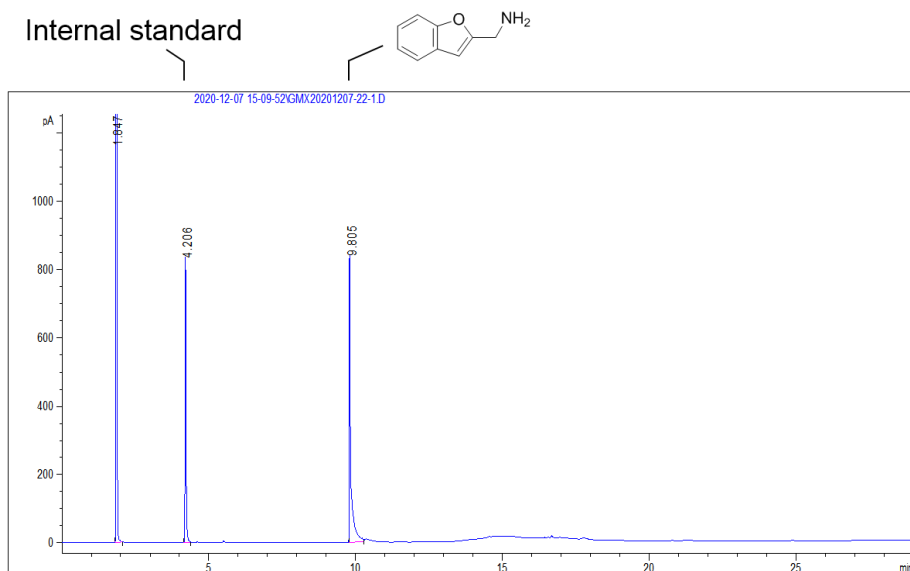


Figure S18. GC spectrum of the reaction mixture (**Figure 7** in the main text). Reaction conditions: 2.0 mmol **1b**, 2 equiv 25% aqueous ammonia, 30 mg Ru/BN-e (0.6 mol%), 7.0 mL MeOH, 1.5 MPa H₂, 90 °C, 2 h.

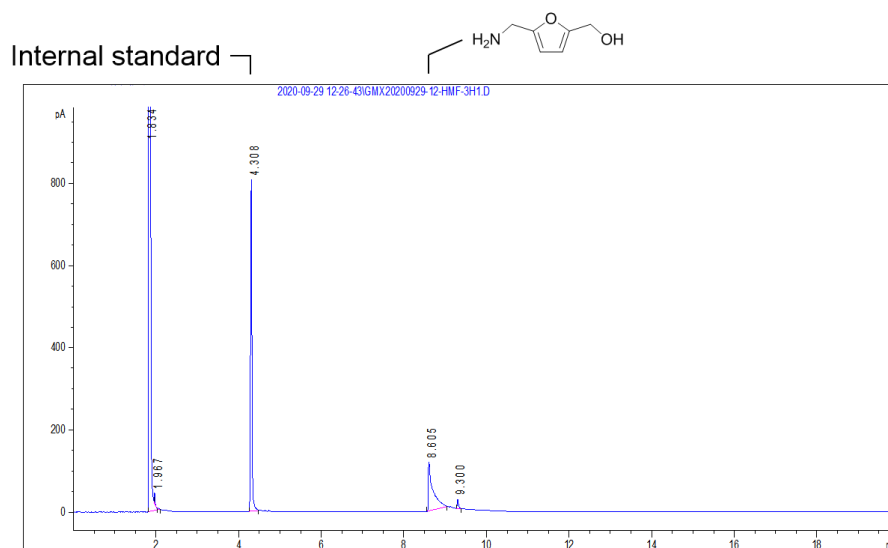


Figure S19. GC spectrum of the reaction mixture (**Figure 7** in the main text). Reaction conditions: 2.0 mmol **1c**, 2 equiv 25% aqueous ammonia, 30 mg Ru/BN-e (0.6 mol%), 7.0 mL MeOH, 1.0 MPa H₂, 90 °C, 3 h.

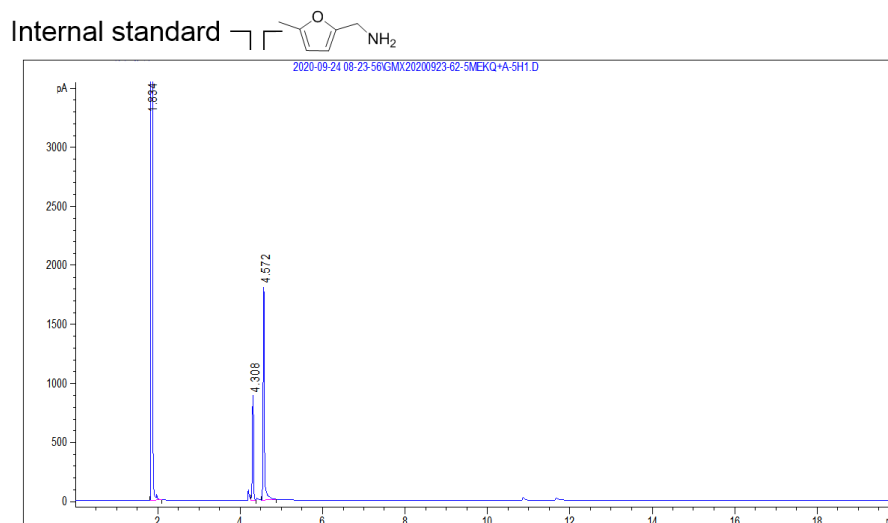


Figure S20. GC spectrum of the reaction mixture (**Figure 7** in the main text). Reaction conditions: 2.0 mmol **1d**, 2.2 mmol **3d**, 2 equiv 25% aqueous ammonia, 30 mg Ru/BN-e (0.6 mol%), 7.0 mL MeOH, 1.0 MPa H₂, 90 °C, 5 h.

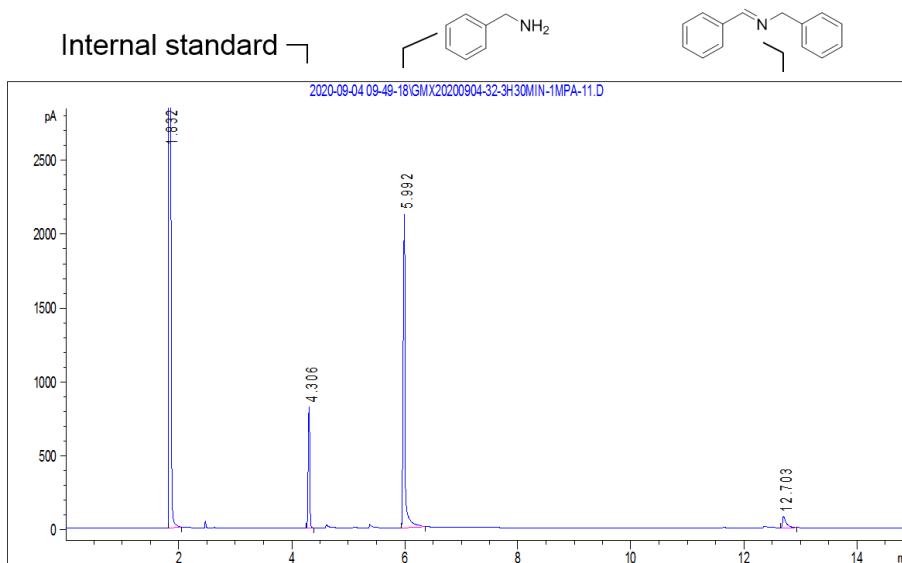


Figure S21. GC spectrum of the reaction mixture (**Figure 7** in the main text). Reaction conditions: 2.0 mmol **1e**, 2.2 mmol **3e**, 2 equiv 25% aqueous ammonia, 30 mg Ru/BN-e (0.6 mol%), 7.0 mL MeOH, 1.0 MPa H₂, 90 °C, 3.5 h.

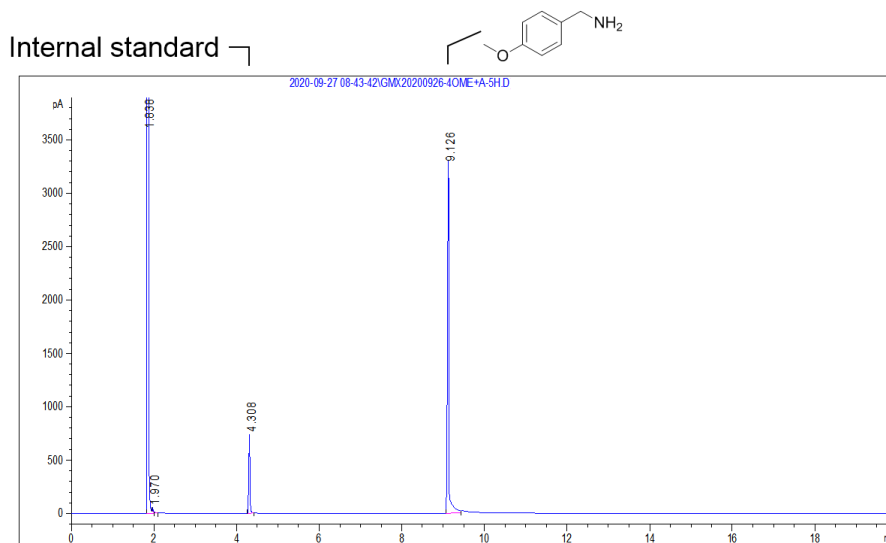


Figure S22. GC spectrum of the reaction mixture (**Figure 7** in the main text). Reaction conditions: 2.0 mmol **1f**, 2.2 mmol **3f**, 2 equiv 25% aqueous ammonia, 30 mg Ru/BN-e (0.6 mol%), 7.0 mL MeOH, 1.0 MPa H₂, 90 °C, 5 h.

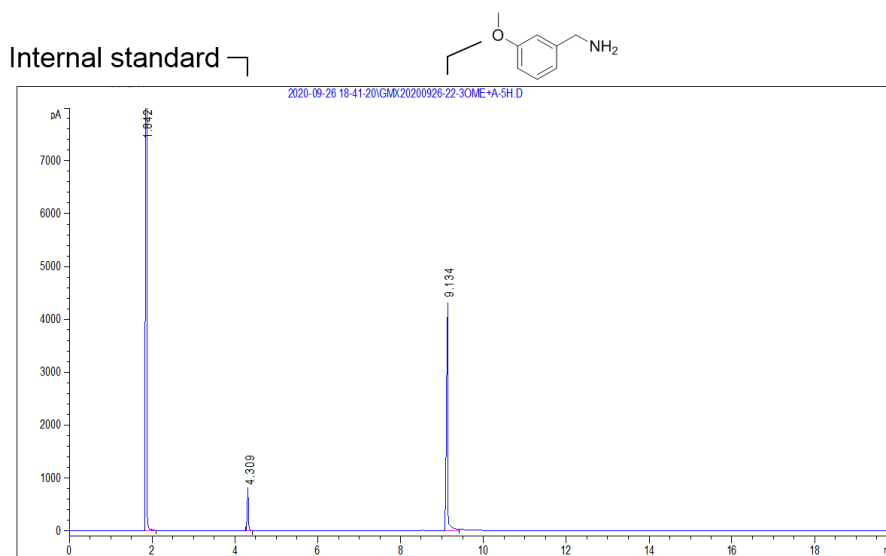


Figure S23. GC spectrum of the reaction mixture (**Figure 7** in the main text). Reaction conditions: 2.0 mmol **1g**, 2.2 mmol **3g**, 2 equiv 25% aqueous ammonia, 30 mg Ru/BN-e (0.6 mol%), 7.0 mL MeOH, 1.0 MPa H₂, 90 °C, 5 h.

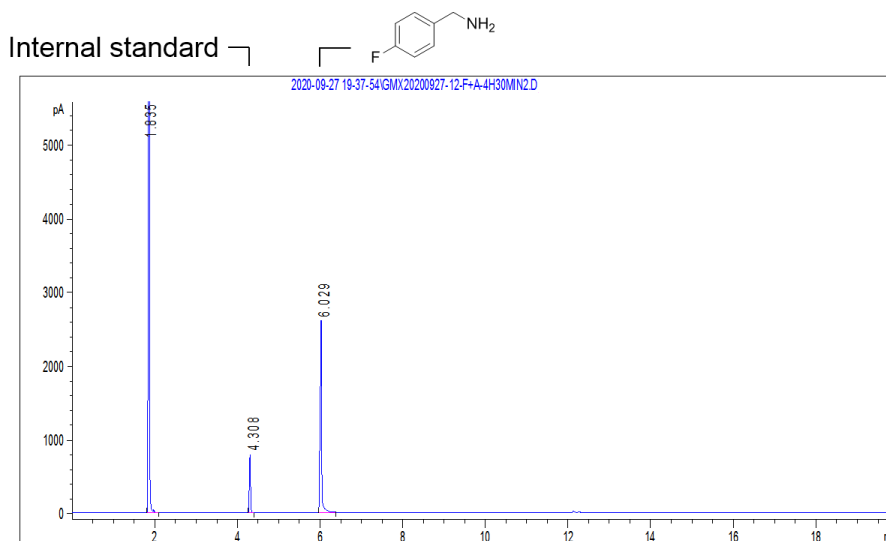


Figure S24. GC spectrum of the reaction mixture (**Figure 7** in the main text). Reaction conditions: 2.0 mmol **1h**, 2.2 mmol **3h**, 2 equiv 25% aqueous ammonia, 30 mg Ru/BN-e (0.6 mol%), 7.0 mL MeOH, 1.0 MPa H₂, 90 °C, 4.5 h.

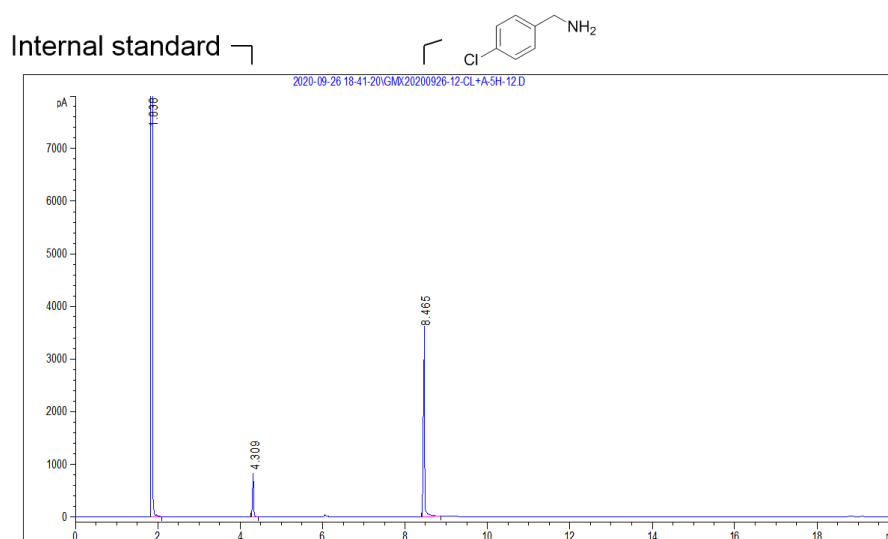


Figure S25. GC spectrum of the reaction mixture (**Figure 7** in the main text). Reaction conditions: 2.0 mmol **1i**, 2.2 mmol **3i**, 2 equiv 25% aqueous ammonia, 30 mg Ru/BN-e (0.6 mol%), 7.0 mL MeOH, 1.0 MPa H₂, 90 °C, 5 h.

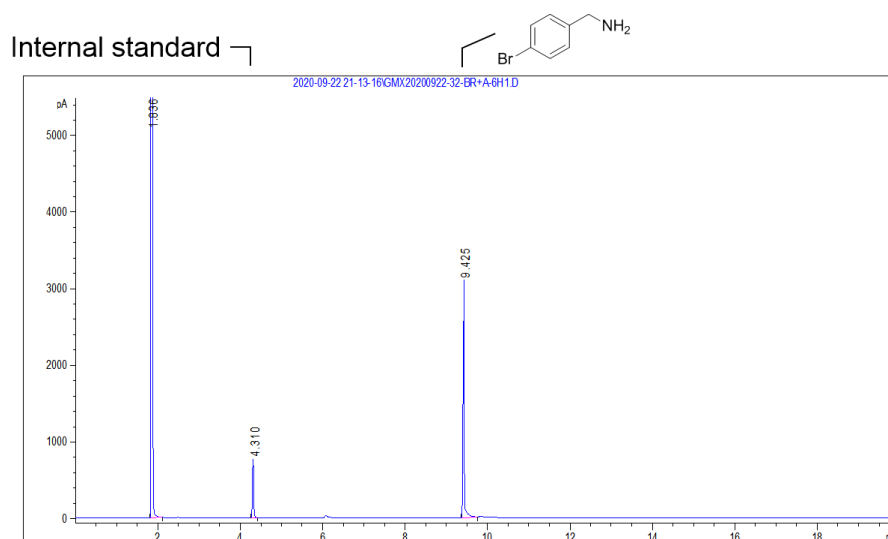


Figure S26. GC spectrum of the reaction mixture (**Figure 7** in the main text). Reaction conditions: 2.0 mmol **1j**, 2.2 mmol **3j**, 2 equiv 25% aqueous ammonia, 30 mg Ru/BN-e (0.6 mol%), 7.0 mL MeOH, 1.0 MPa H₂, 90 °C, 6 h.

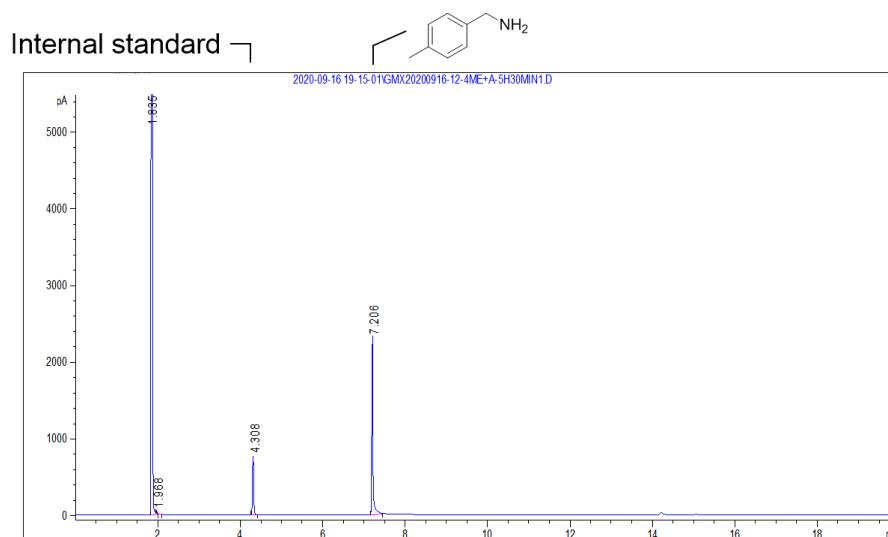


Figure S27. GC spectrum of the reaction mixture (**Figure 7** in the main text). Reaction conditions: 2.0 mmol **1k**, 2.2 mmol **3k**, 2 equiv 25% aqueous ammonia, 30 mg Ru/BN-e (0.6 mol%), 7.0 mL MeOH, 1.0 MPa H₂, 90 °C, 5.5 h.

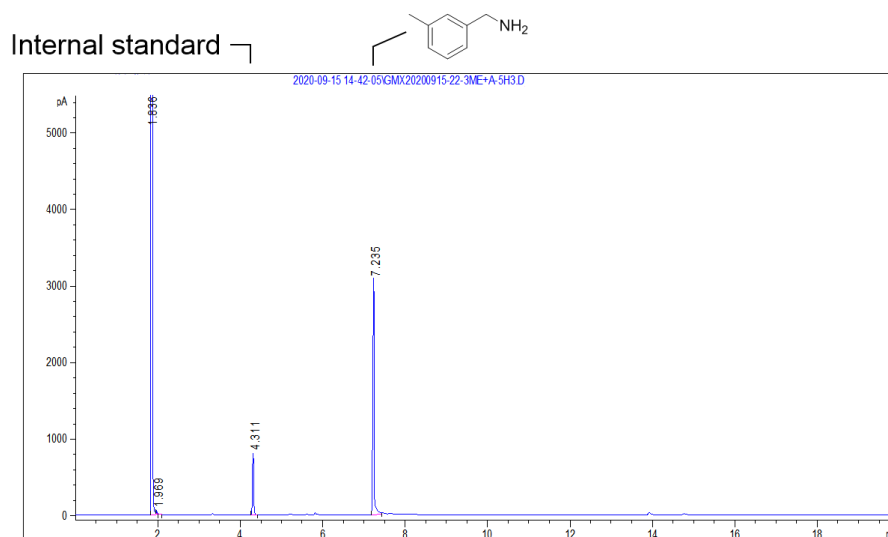


Figure S28. GC spectrum of the reaction mixture (**Figure 7** in the main text). Reaction conditions: 2.0 mmol **1l**, 2.2 mmol **3l**, 2 equiv 25% aqueous ammonia, 30 mg Ru/BN-e (0.6 mol%), 7.0 mL MeOH, 1.0 MPa H₂, 90 °C, 5 h.

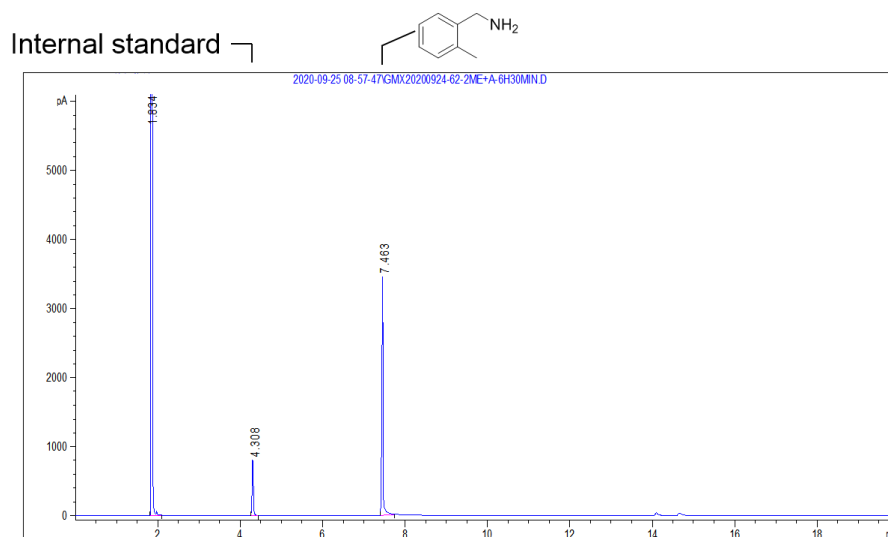


Figure S29. GC spectrum of the reaction mixture (**Figure 7** in the main text). Reaction conditions: 2.0 mmol **1m**, 2.2 mmol **3m**, 2 equiv 25% aqueous ammonia, 30 mg Ru/BN-e (0.6 mol%), 7.0 mL MeOH, 1.0 MPa H₂, 90 °C, 6.5 h.

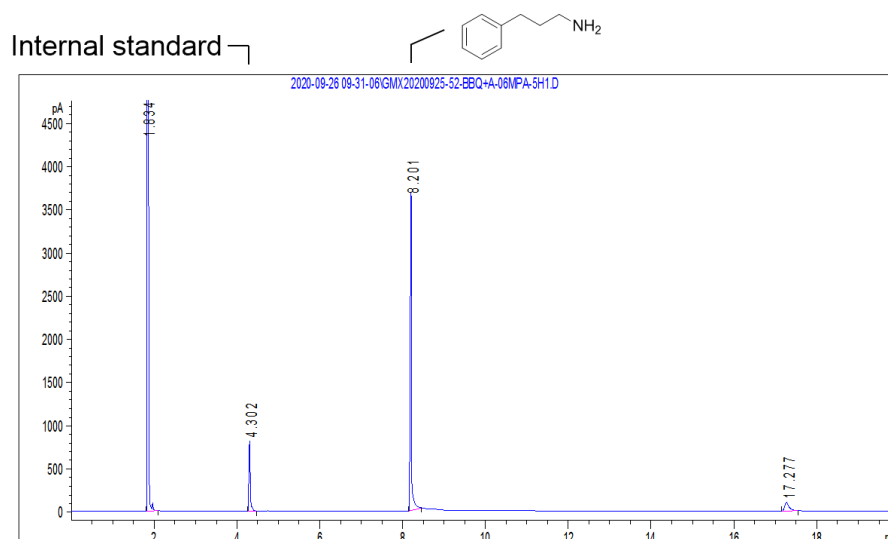


Figure S30. GC spectrum of the reaction mixture (**Figure 7** in the main text). Reaction conditions: 2.0 mmol **1n**, 2.2 mmol **3n**, 2 equiv 25% aqueous ammonia, 30 mg Ru/BN-e (0.6 mol%), 7.0 mL MeOH, 0.6 MPa H₂, 90 °C, 5 h.

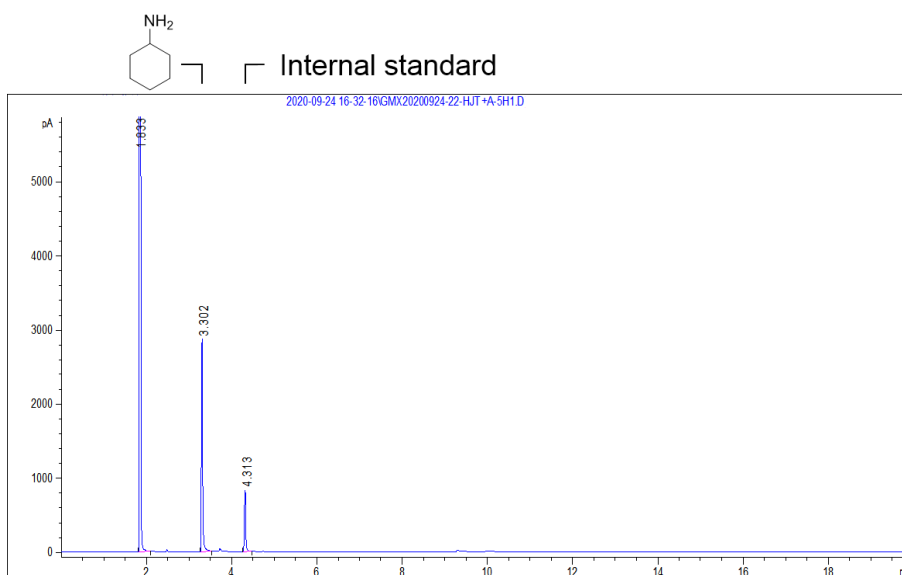


Figure S31. GC spectrum of the reaction mixture (**Figure 7** in the main text). Reaction conditions: 2.0 mmol **1o**, 2.2 mmol **3o**, 2 equiv 25% aqueous ammonia, 30 mg Ru/BN-e (0.6 mol%), 7.0 mL MeOH, 1.0 MPa H₂, 90 °C, 5 h.

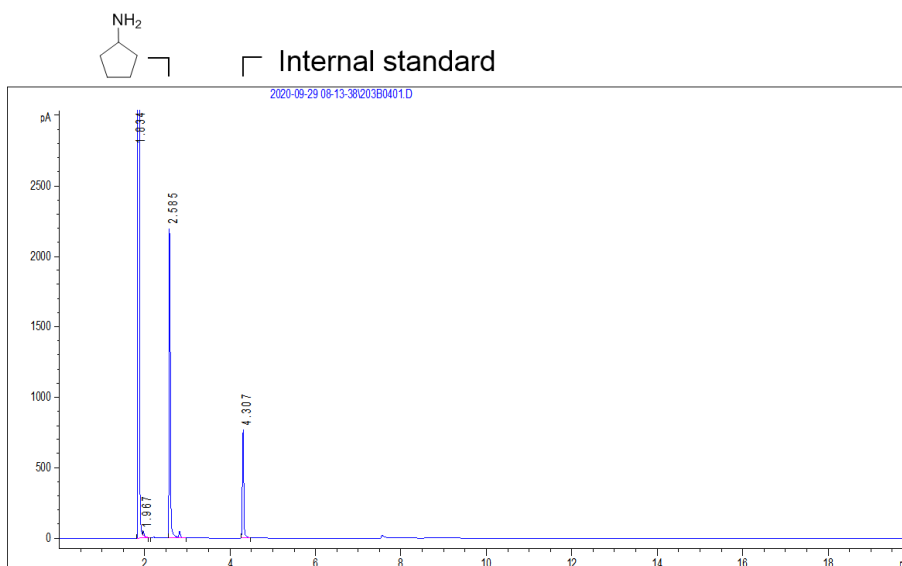


Figure S32. GC spectrum of the reaction mixture (**Figure 7** in the main text). Reaction conditions: 2.0 mmol **1p**, 2.2 mmol **3p**, 2 equiv 25% aqueous ammonia, 30 mg Ru/BN-e (0.6 mol%), 7.0 mL MeOH, 1.0 MPa H₂, 90 °C, 12 h.

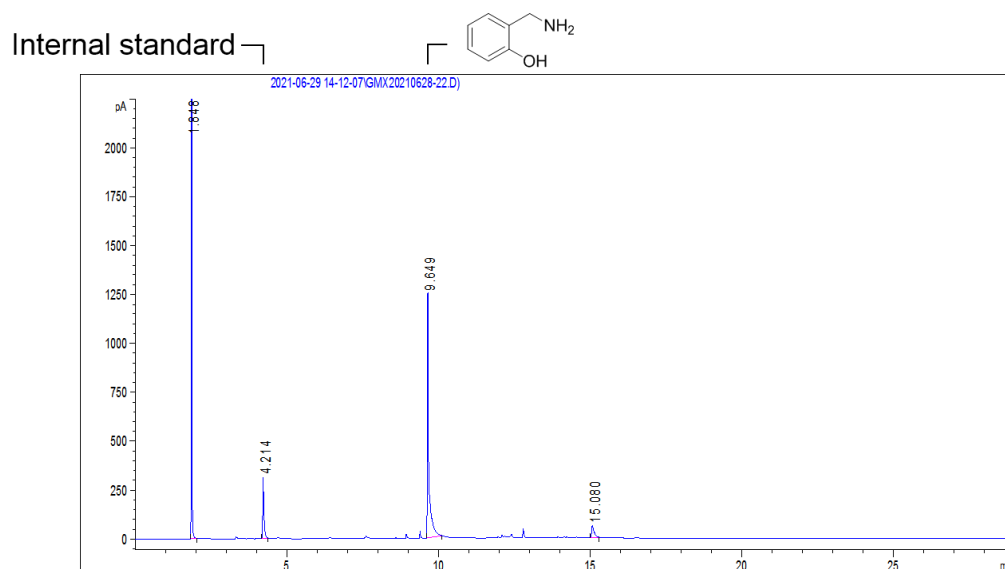


Figure S33. GC spectrum of the reaction mixture (**Figure 7** in the main text). Reaction conditions: 2.0 mmol **1q**, 2.2 mmol **3q**, 2 equiv 25% aqueous ammonia, 30 mg Ru/BN-e (0.6 mol%), 7.0 mL MeOH, 1.5 MPa H₂, 90 °C, 12 h.

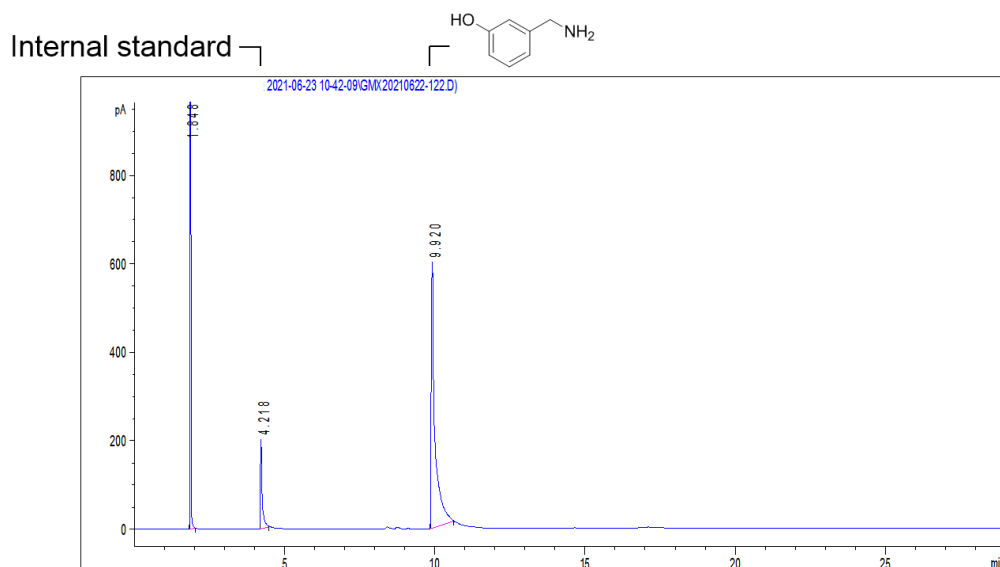


Figure S34. GC spectrum of the reaction mixture (**Figure 7** in the main text). Reaction conditions: 2.0 mmol **1r**, 2.2 mmol **3r**, 2 equiv 25% aqueous ammonia, 30 mg Ru/BN-e (0.6 mol%), 7.0 mL MeOH, 1.0 MPa H₂, 90 °C, 7 h.

Internal standard

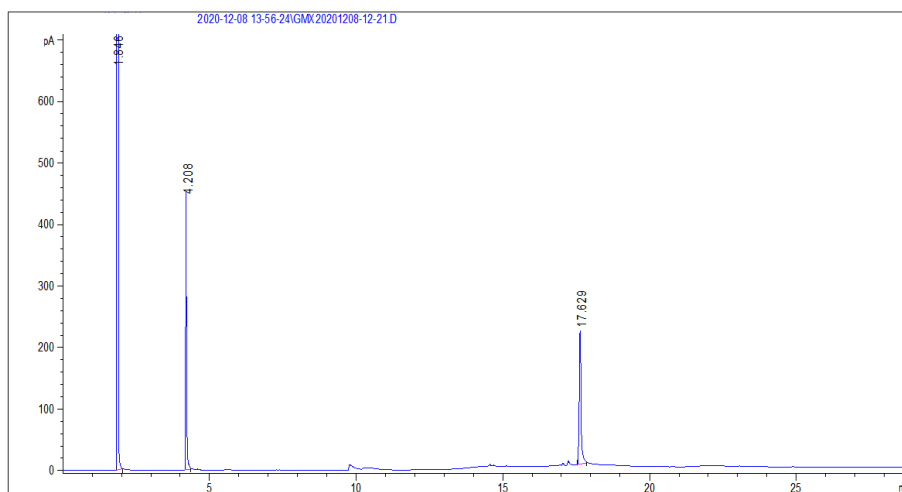
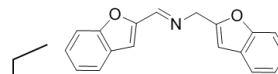


Figure S35. GC spectrum of the reaction mixture (**Figure S12** in the supplementary materials). Reaction conditions: 2.0 mmol **1b**, 2 equiv 25% aqueous ammonia, 30 mg Ru/BN-b (0.6 mol%), 7.0 mL MeOH, 1.5 MPa H₂, 90 °C, 2 h.

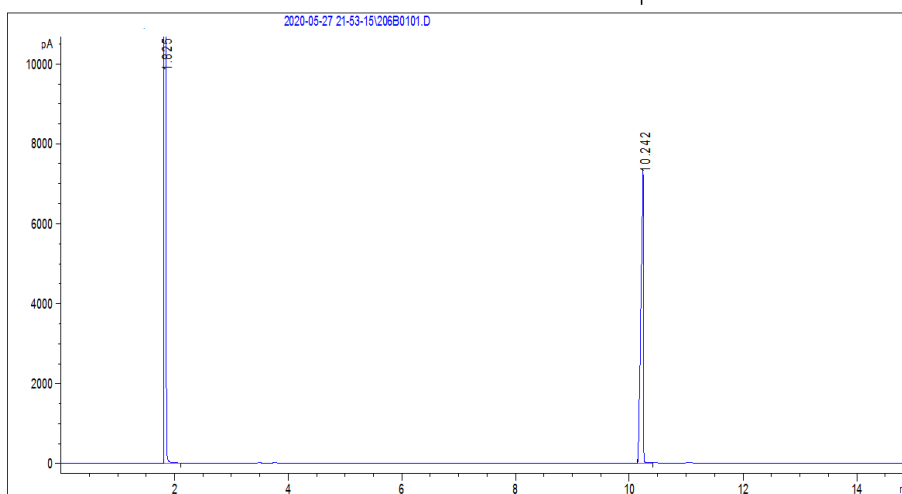
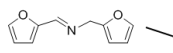


Figure S36. GC spectrum of the reaction mixture for synthesis of N-furfurylidene-furfurylamine (**4a**). Reaction conditions: 2.0 mmol **1a**, 2.0 mmol **3a**, 7.0 mL MeOH, 30 °C, 2 h.

MS: m/z (%): 95 (2) [M+], 40 (3), 32 (30), 28 (100)

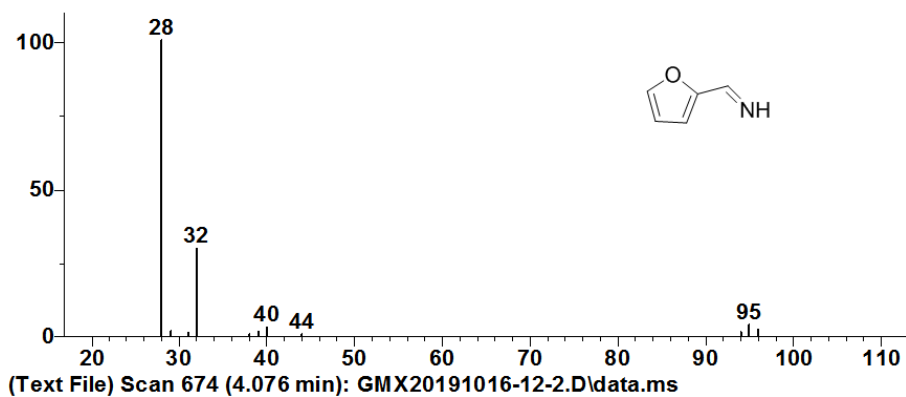


Figure S37. The MS spectrum of furfurylimine (**2a**).

MS: m/z (%): 97 (92) [M+], 81 (37), 69 (100), 53 (33), 41 (34)

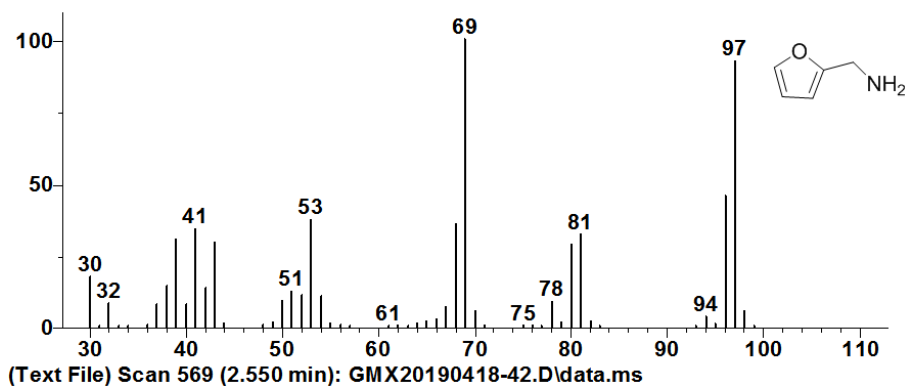


Figure S38. The MS spectrum of furfurylamine (**3a**).

MS: m/z (%): 175 (12) [M+], 81 (35), 53 (9), 40 (10), 32 (100)

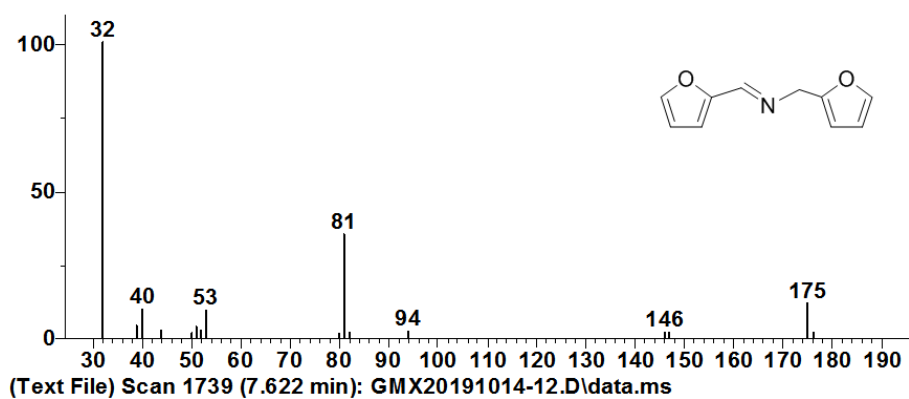


Figure S39. The MS spectrum of N-furfurylidene-furfurylamine (**4a**).

MS: m/z (%): 268 (18) [M+], 173 (23), 52 (9), 40 (9), 32 (100)

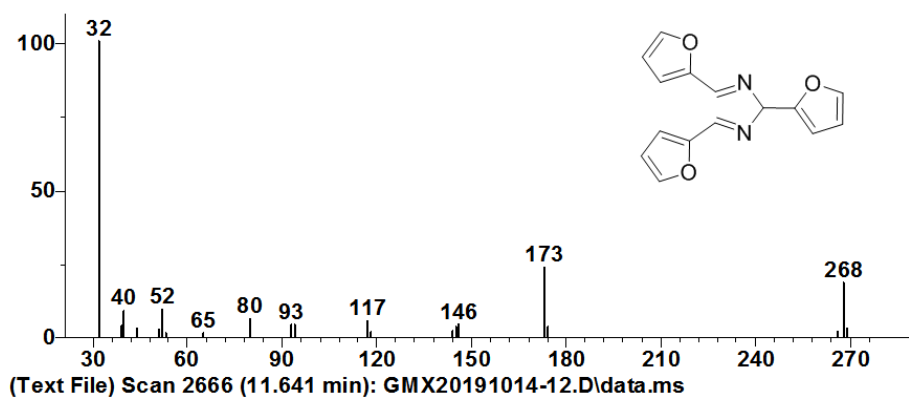


Figure S40. The MS spectrum of hydrofufamide (**5a**).

MS: m/z (%): 268 (75) [M+], 173 (100), 117 (24), 80 (24), 52 (37)

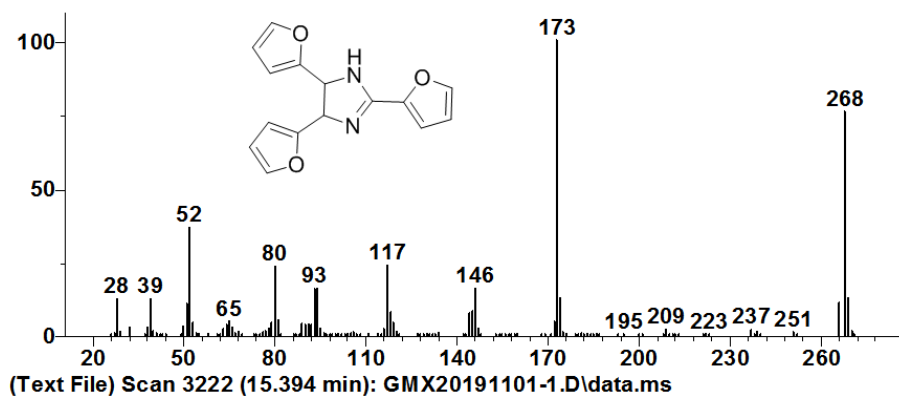


Figure S41. The MS spectrum of 2,4,5-tris(2-furyl)imidazoline.

MS: m/z (%): 147 (58) [M+], 146 (96), 130 (100), 118 (14), 91 (35)

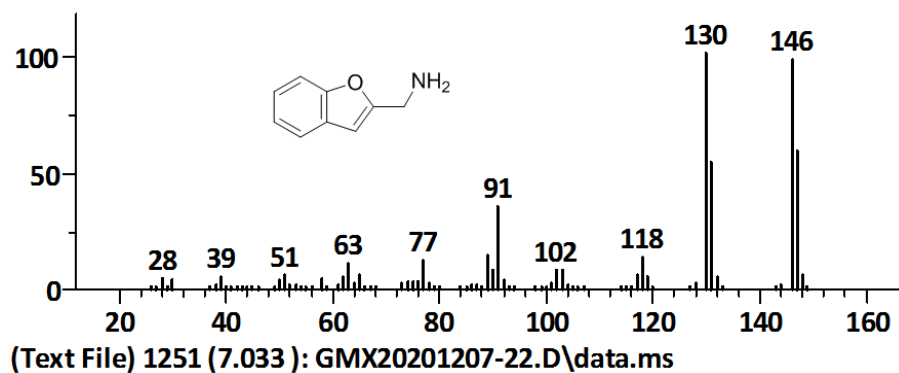


Figure S42. The MS spectrum of 2-benzofuranmethanamine (**3b**).

MS: m/z (%): 127 (22) [M+], 96 (100), 68 (15), 41 (17), 28 (83)

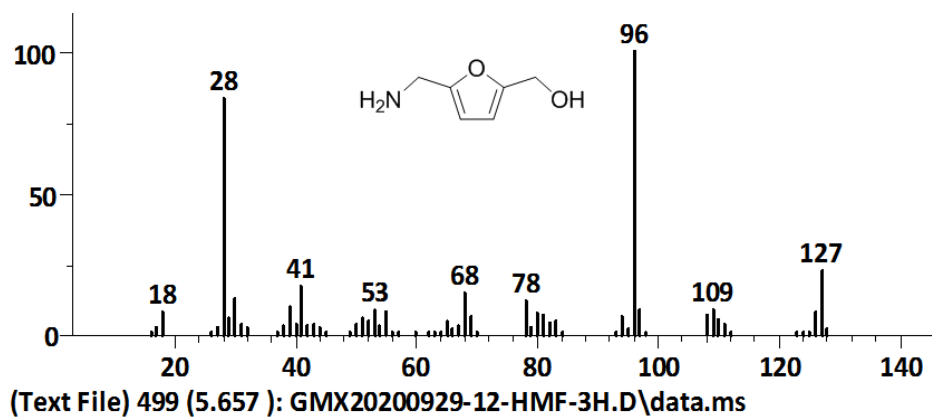


Figure S43. The MS spectrum of (5-aminomethyl-furan-2-yl)-methanol (**3c**).

MS: m/z (%): 111 (91) [M+], 96 (100), 83 (26), 78 (25), 68 (37)

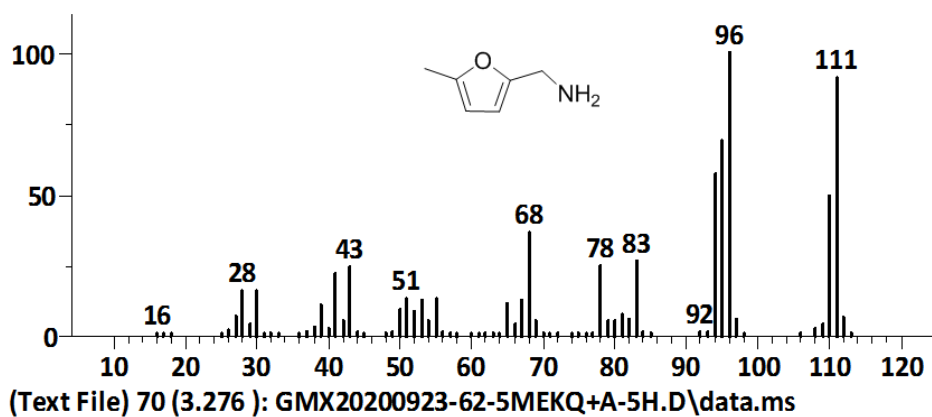


Figure S44. The MS spectrum of 5-Methylfurfurylamine (**3d**).

MS: m/z (%): 107 (57) [M+], 106 (100), 91 (12), 79 (33), 51 (10)

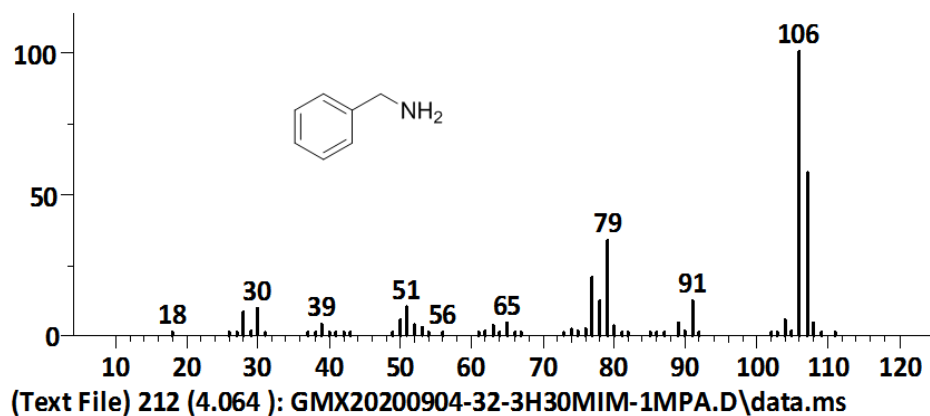


Figure S45. The MS spectrum of benzylamine (3e).

MS: m/z (%): 137 (54) [M+], 136 (100), 121 (42), 106 (42), 77 (21)

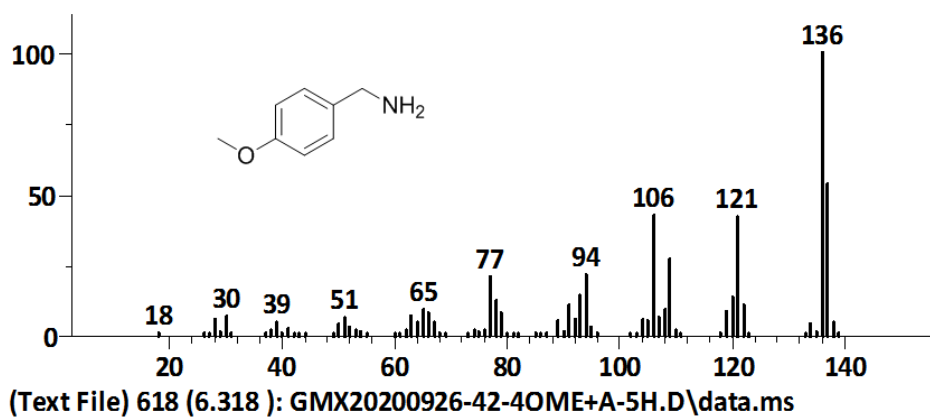


Figure S46. The MS spectrum of 4-Methoxybenzylamine (3f).

MS: m/z (%): 137 (64) [M+], 136 (100), 106 (47), 94 (26), 77 (24)

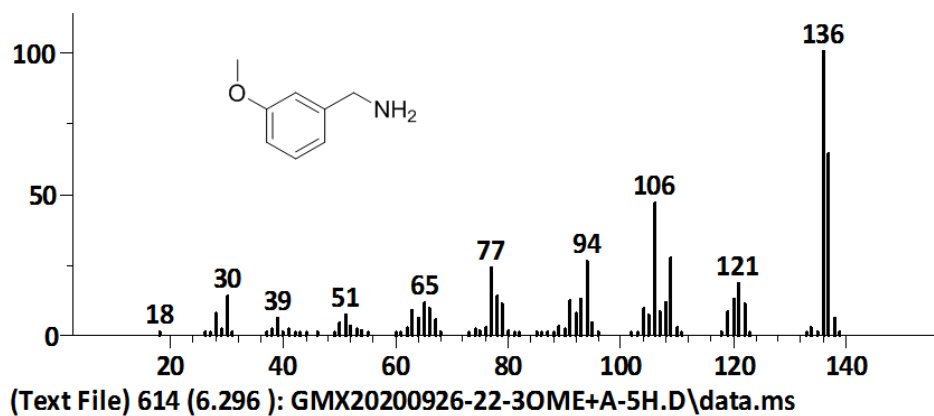


Figure S47. The MS spectrum of 3-Methoxybenzylamine (**3g**).

MS: m/z (%): 125 (35) [M+], 124 (100), 105 (45), 97 (34), 28 (22)

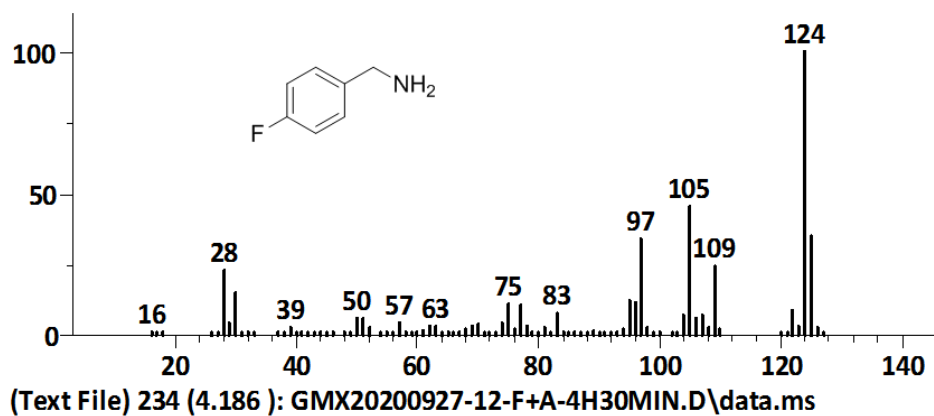


Figure S48. The MS spectrum of 4-Fluorobenzylamine (**3h**).

MS: m/z (%): 141 (14) [M+], 140 (53), 106 (100), 77 (28), 28 (13)

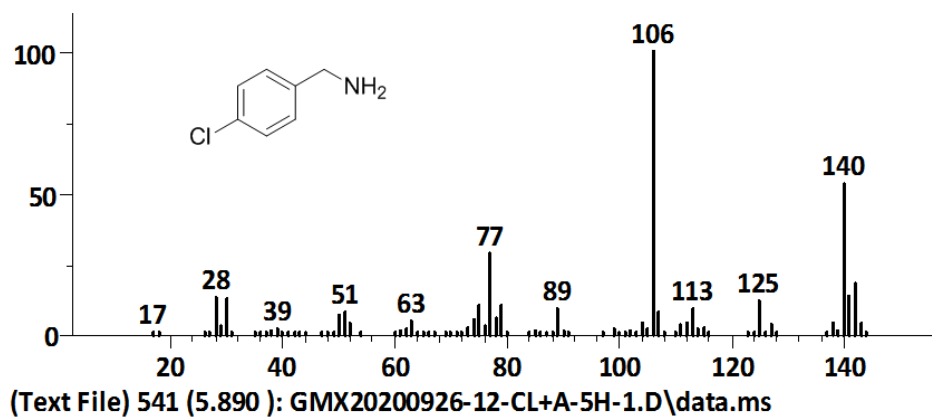


Figure S49. The MS spectrum of 4-Chlorobenzaldehyde (**3i**).

MS: m/z (%): 186 (35) [M+], 184 (38), 157 (7), 106 (100), 77 (21)

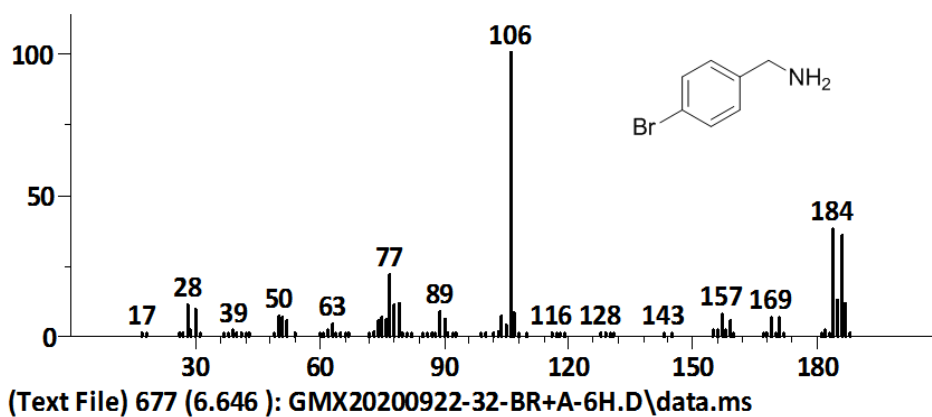


Figure S50. The MS spectrum of 4-Bromobenzaldehyde (**3j**).

MS: m/z (%): 121 (35) [M+], 120 (76), 104 (100), 91 (52), 77 (29)

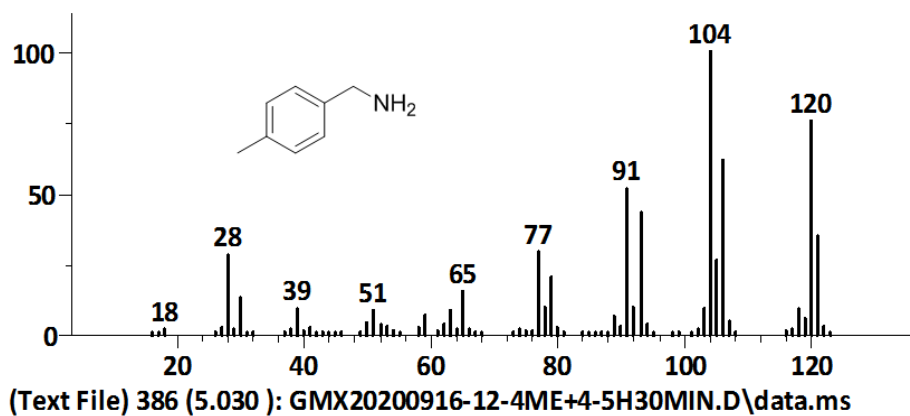


Figure S51. The MS spectrum of 4-Methylbenzylamine (**3k**).

MS: m/z (%): 121 (32) [M+], 120 (76), 104 (100), 91 (49), 77 (27)

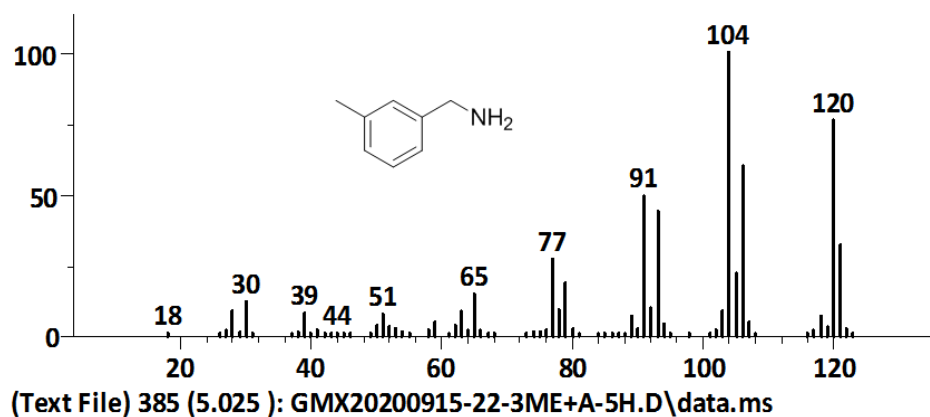


Figure S52. The MS spectrum of 3-Methylbenzylamine (**3l**).

MS: m/z (%): 121 (11) [M+], 120 (17), 104 (100), 91 (23), 77 (16)

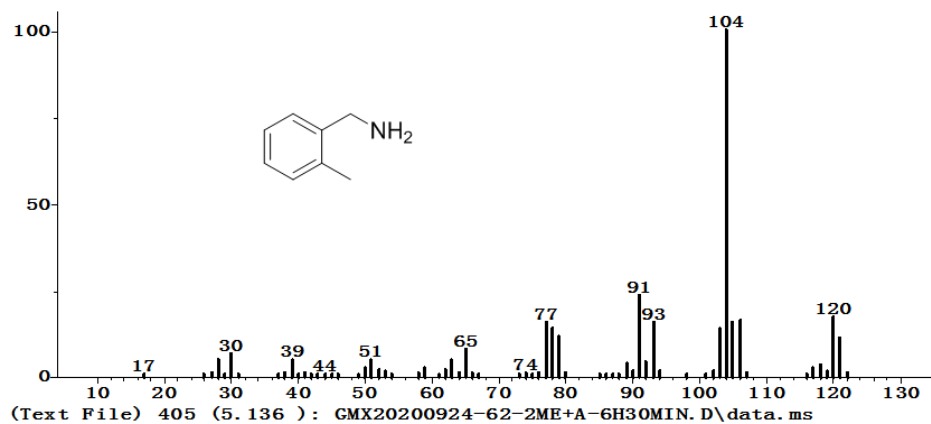


Figure S53. The MS spectrum of 2-Methylbenzylamine (**3m**).

MS: m/z (%): 135 (5) [M+], 118 (100), 91 (35), 77 (12), 30 (45)

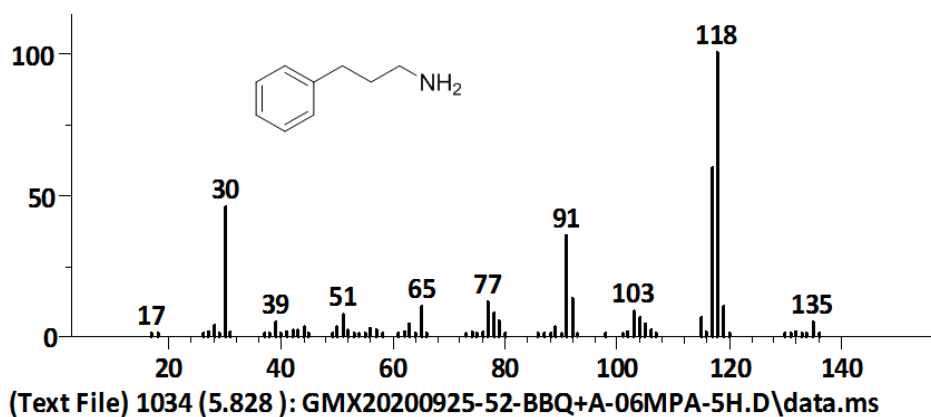


Figure S54. The MS spectrum of 3-Phenyl-1-propylamine (**3n**).

MS: m/z (%): 99 (18) [M+], 70 (9), 56 (100), 43 (19), 28 (10)

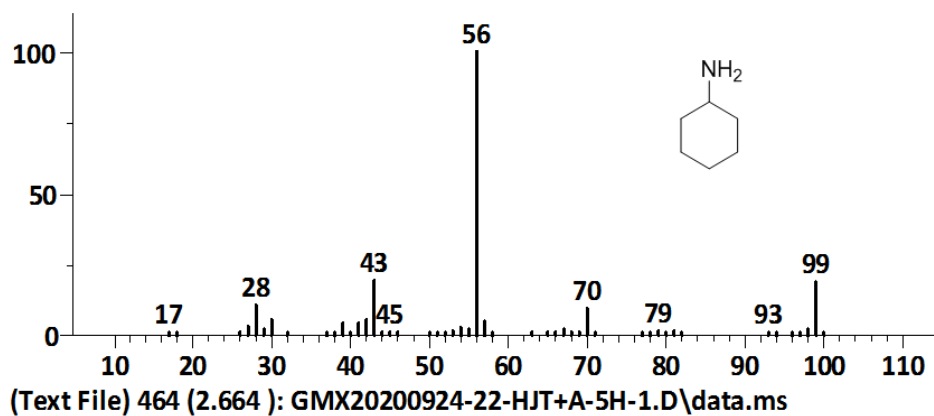


Figure S55. The MS spectrum of cyclohexylamine (**3o**).

MS: m/z (%): 85(16) [M+], 67 (3), 56 (100), 43 (8), 28 (8)

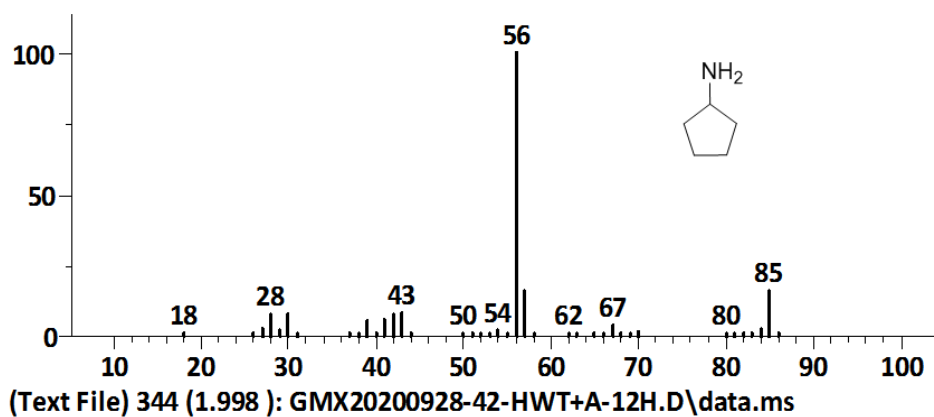


Figure S56. The MS spectrum of cyclopentylamine (**3p**).

MS: m/z (%): 123 (88) [M+], 106 (53), 95 (13), 78 (100), 51 (12)

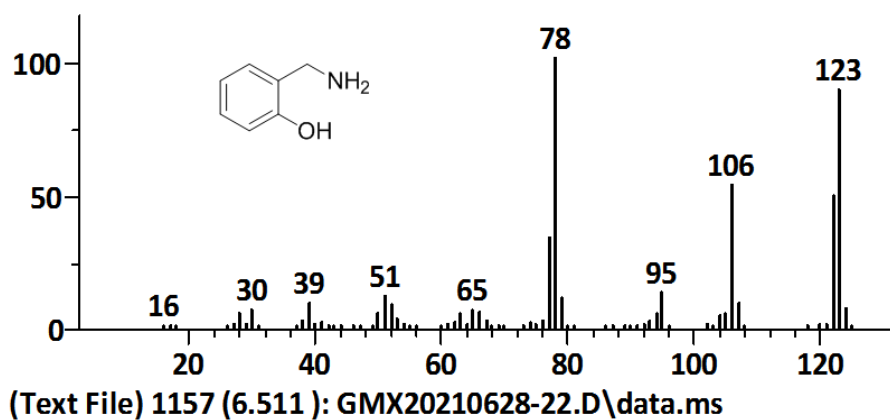


Figure S57. The MS spectrum of 2-hydroxybenzylamine (**3q**).

MS: m/z (%): 123 (88) [M+], 122 (100), 106 (41), 95 (38), 77 (39)

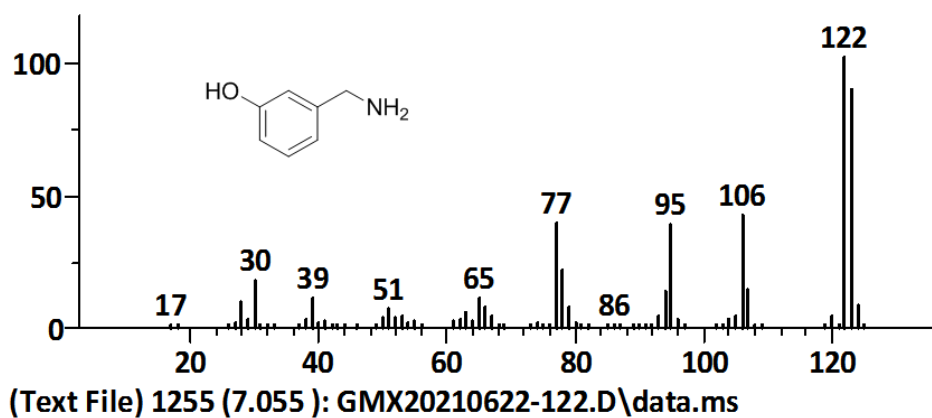


Figure S58. The MS spectrum of 3-hydroxybenzylamine (**3r**).

MS: m/z (%): 275 (36) [M+], 131 (100), 77 (12)

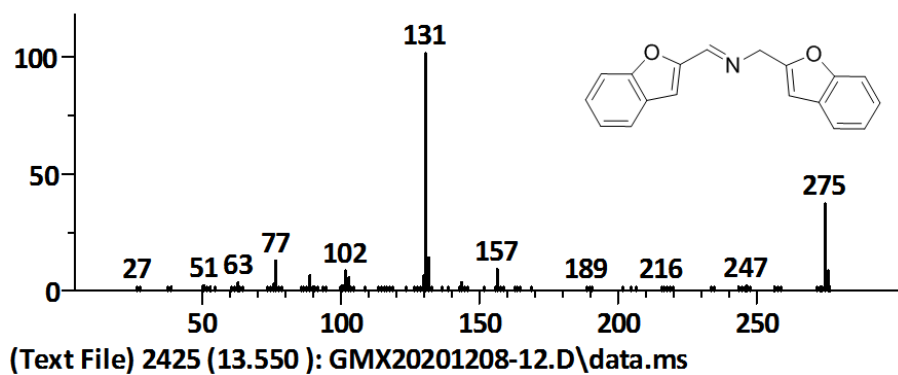


Figure S59. The MS spectrum of 1-(benzofuran-2-yl)-N-[(benzofuran-2-yl)methyl]methanimine (**4b**).

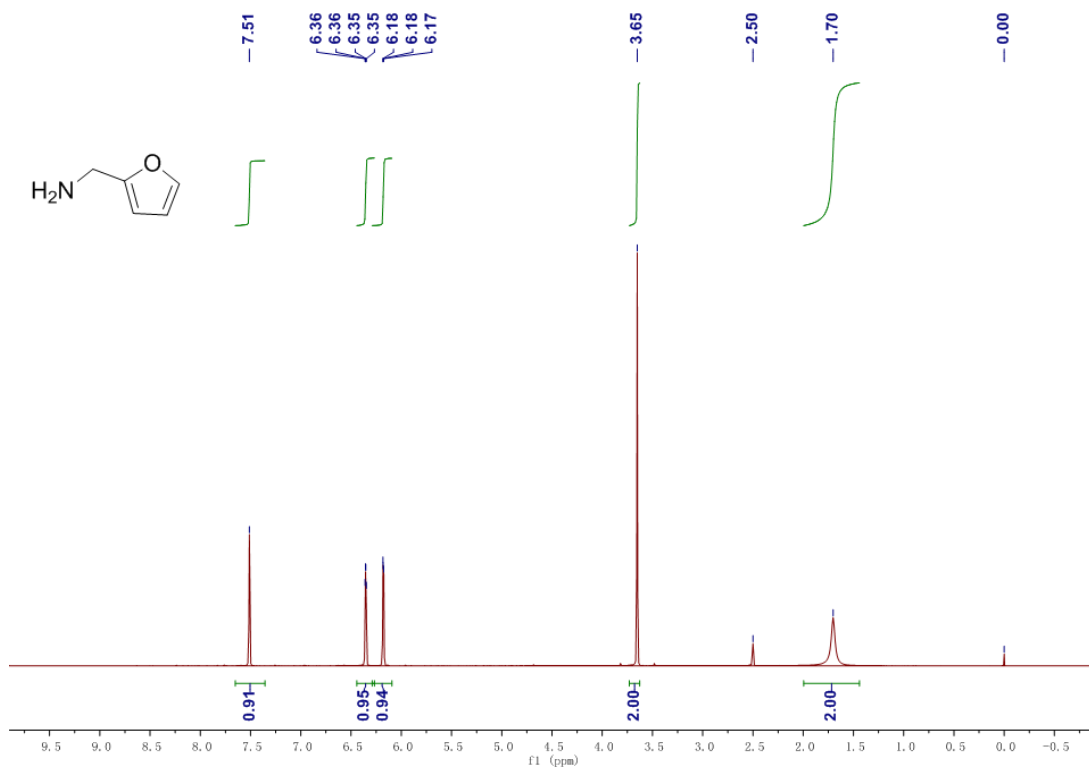


Figure S60. ¹H NMR spectrum of isolated 3a.

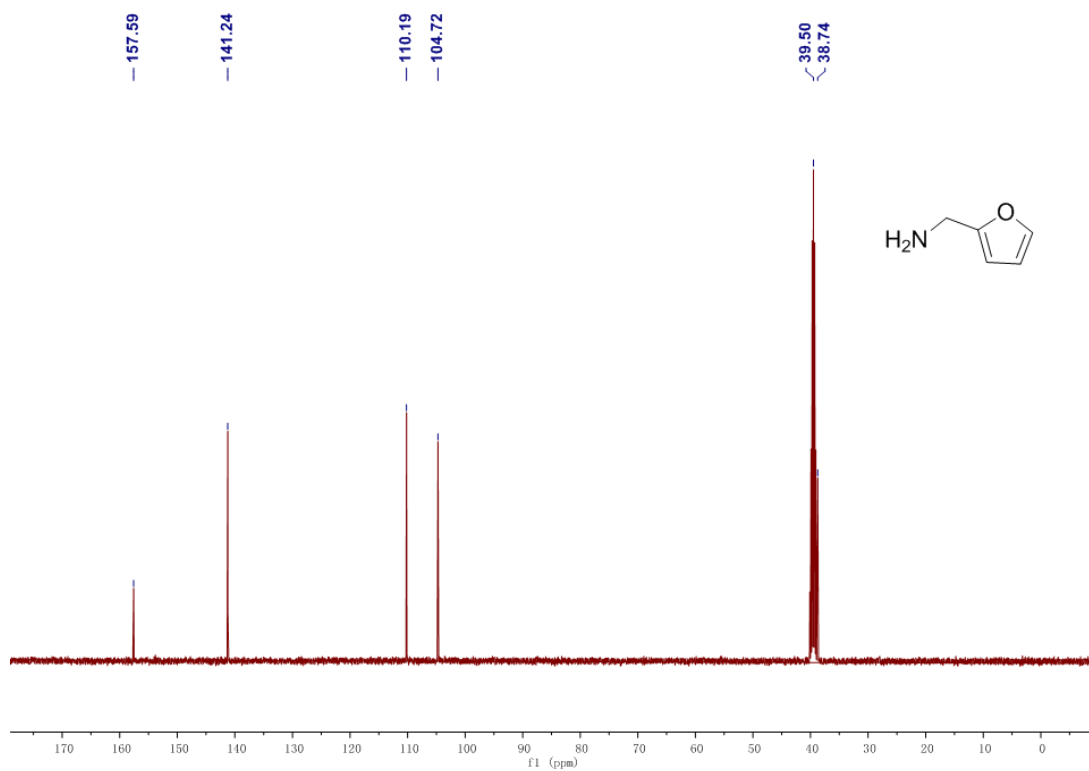


Figure S61. ¹³C NMR spectrum of isolated 3a.

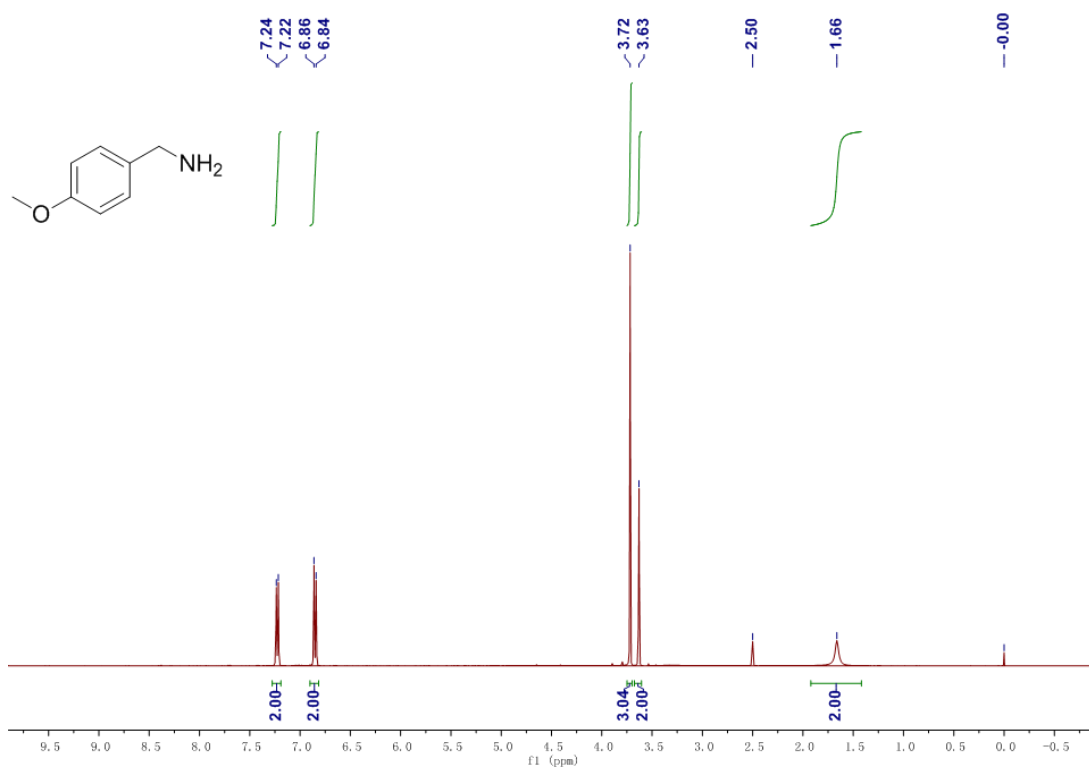


Figure S62. ¹H NMR spectrum of isolated **3f**.

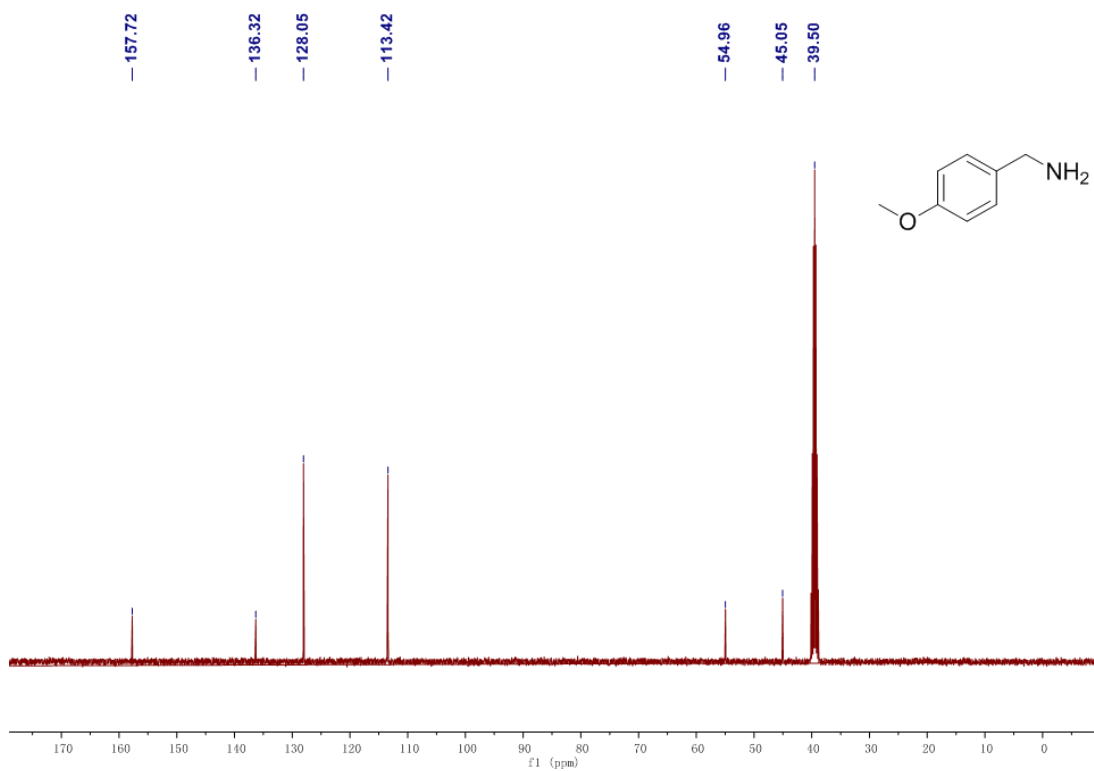


Figure S63. ¹³C NMR spectrum of isolated **3f**.

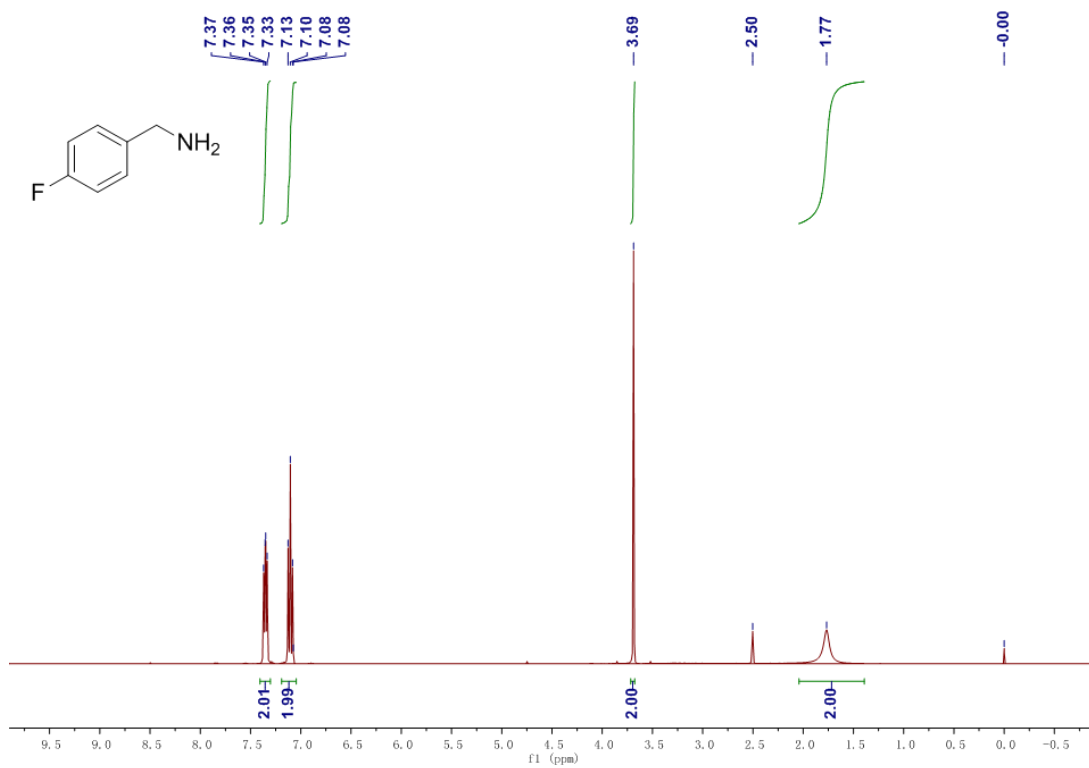


Figure S64. ¹H NMR spectrum of isolated **3h**.

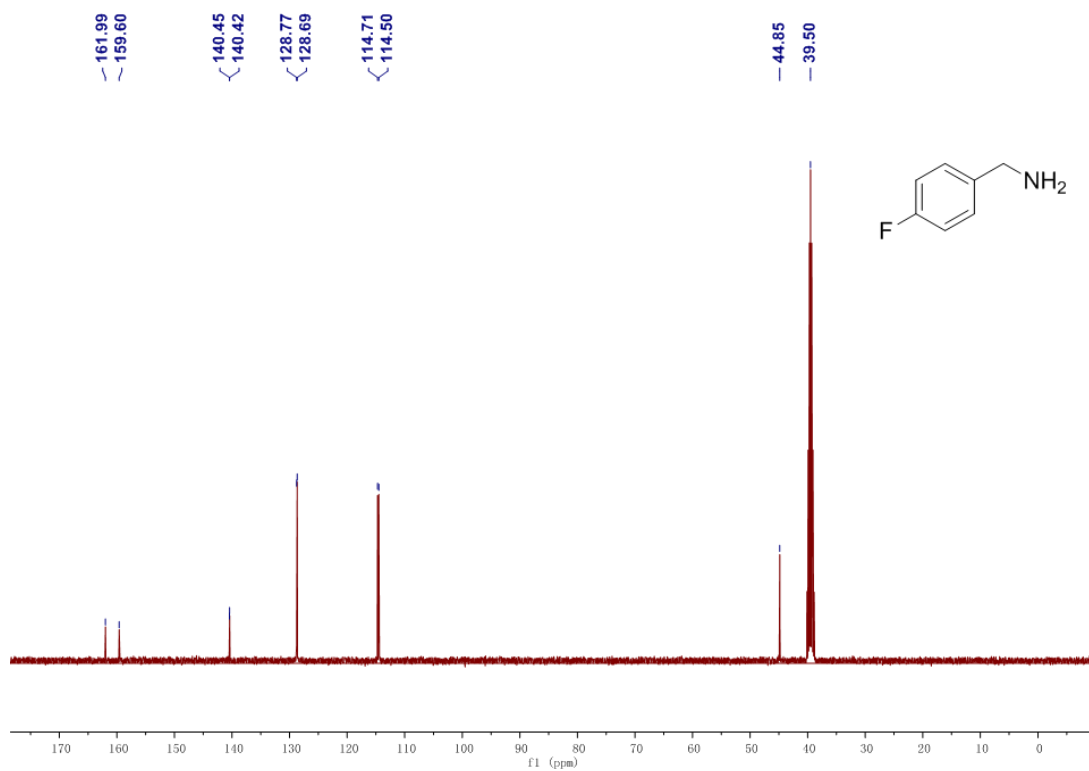


Figure S65. ¹³C NMR spectrum of isolated **3h**.

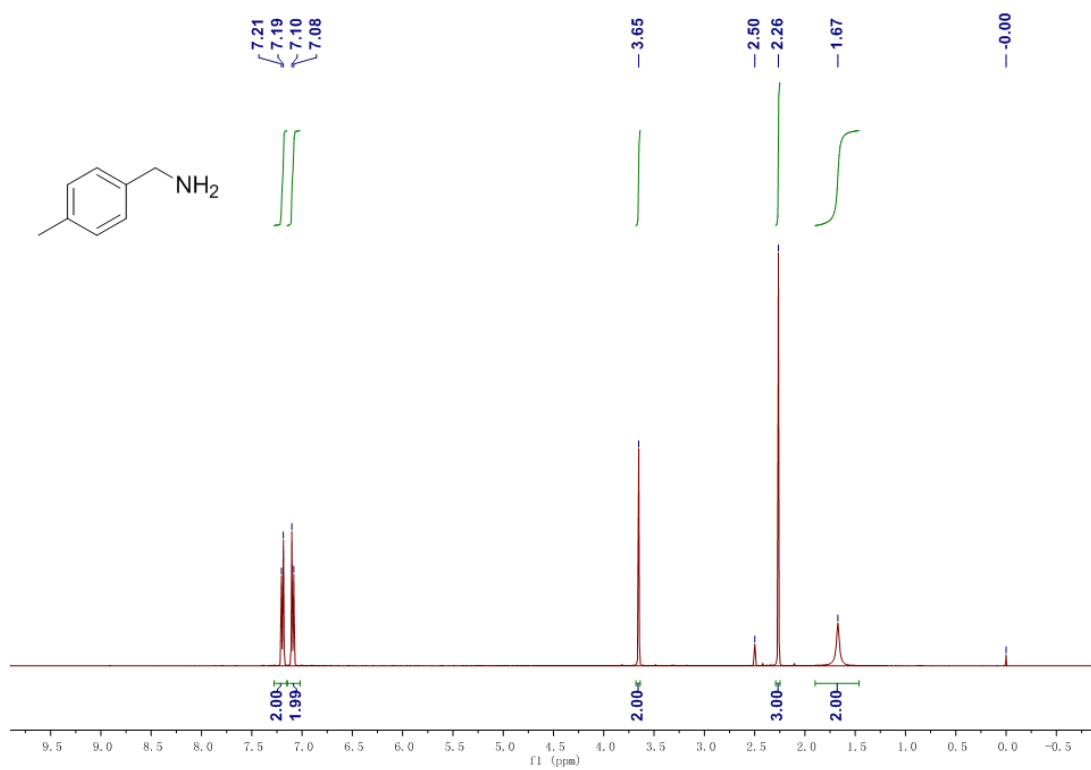


Figure S66. ¹H NMR spectrum of isolated **3k**.

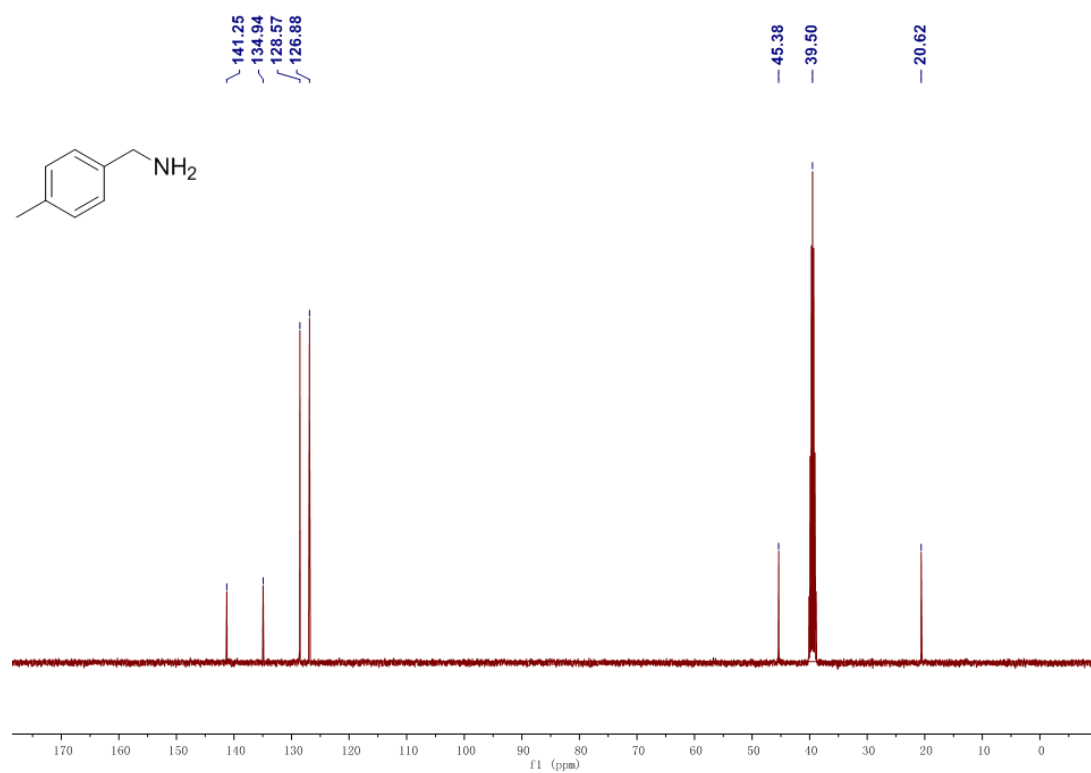


Figure S67. ¹³C NMR spectrum of isolated **3k**.

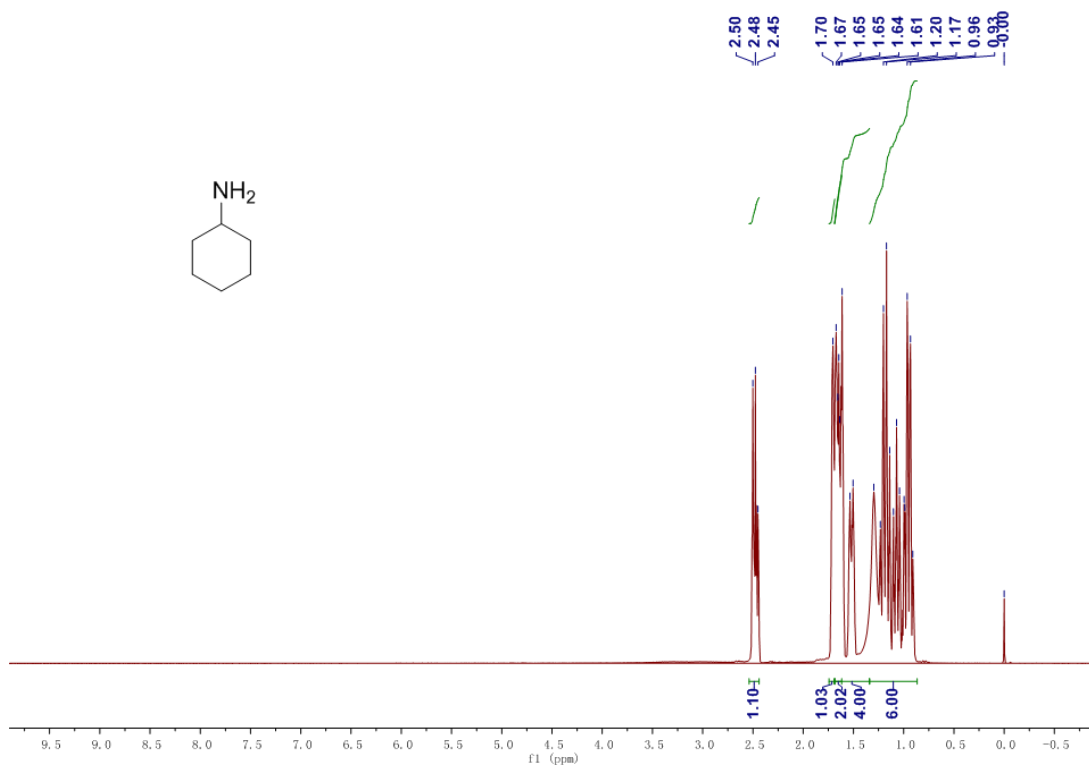


Figure S68. ¹H NMR spectrum of isolated 3o.

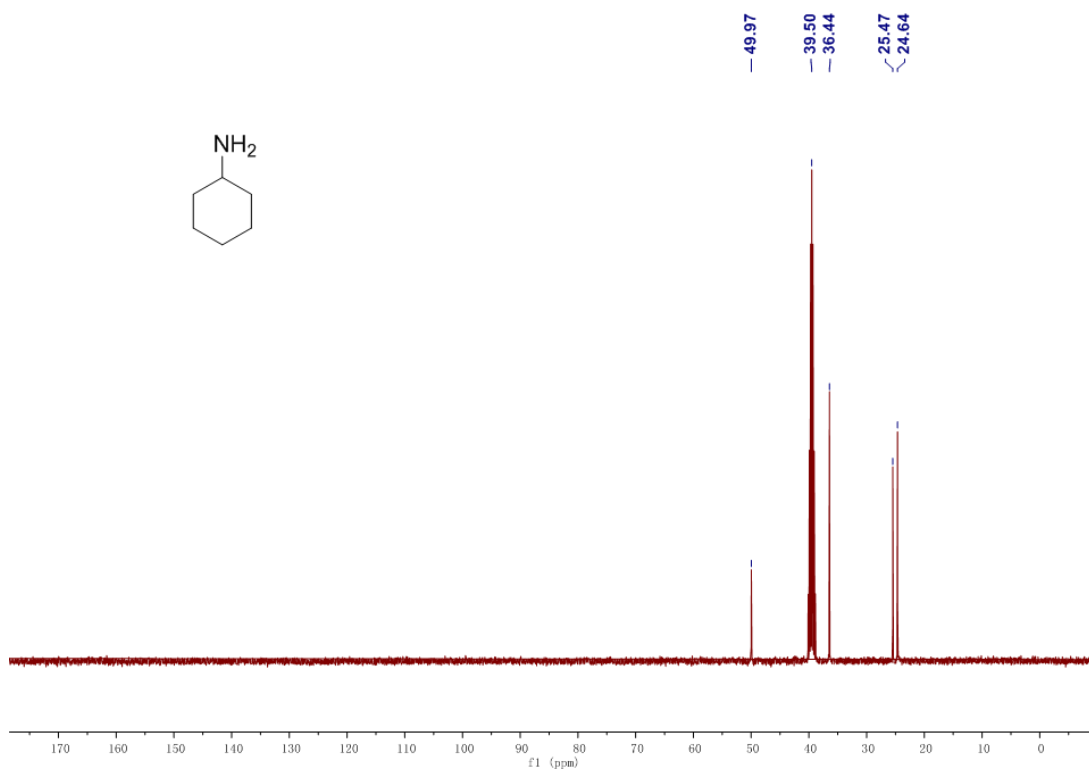


Figure S69. ¹³C NMR spectrum of isolated 3o.

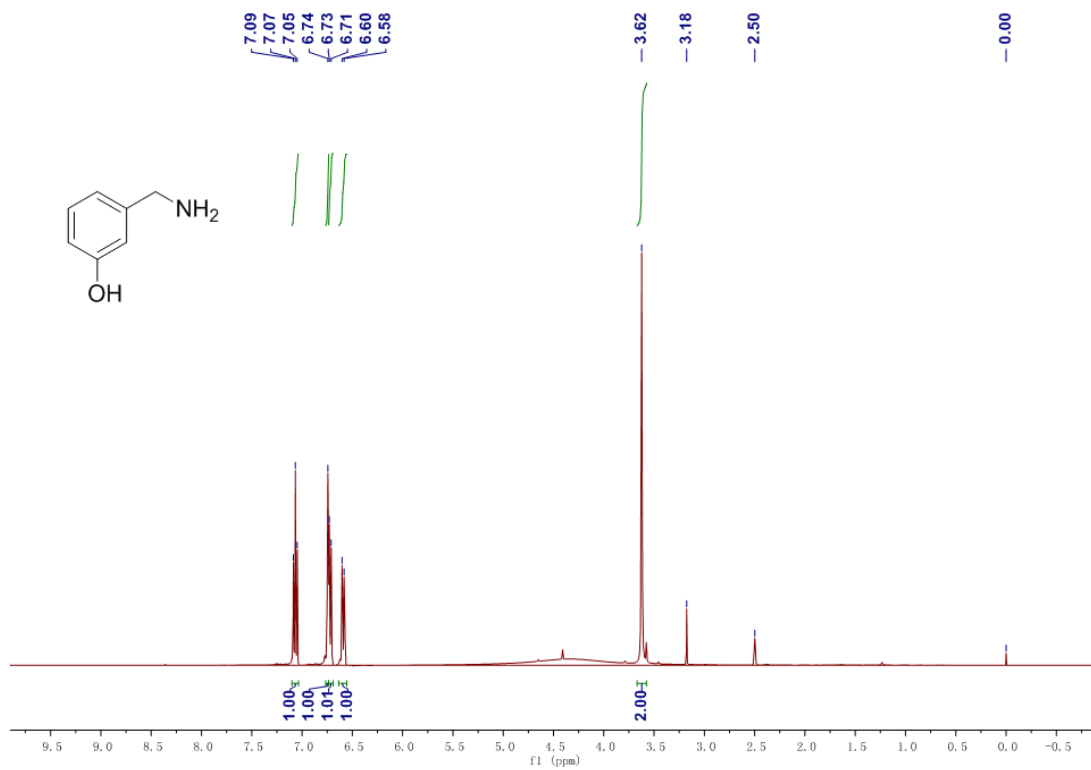


Figure S70. ¹H NMR spectrum of isolated **3r**.

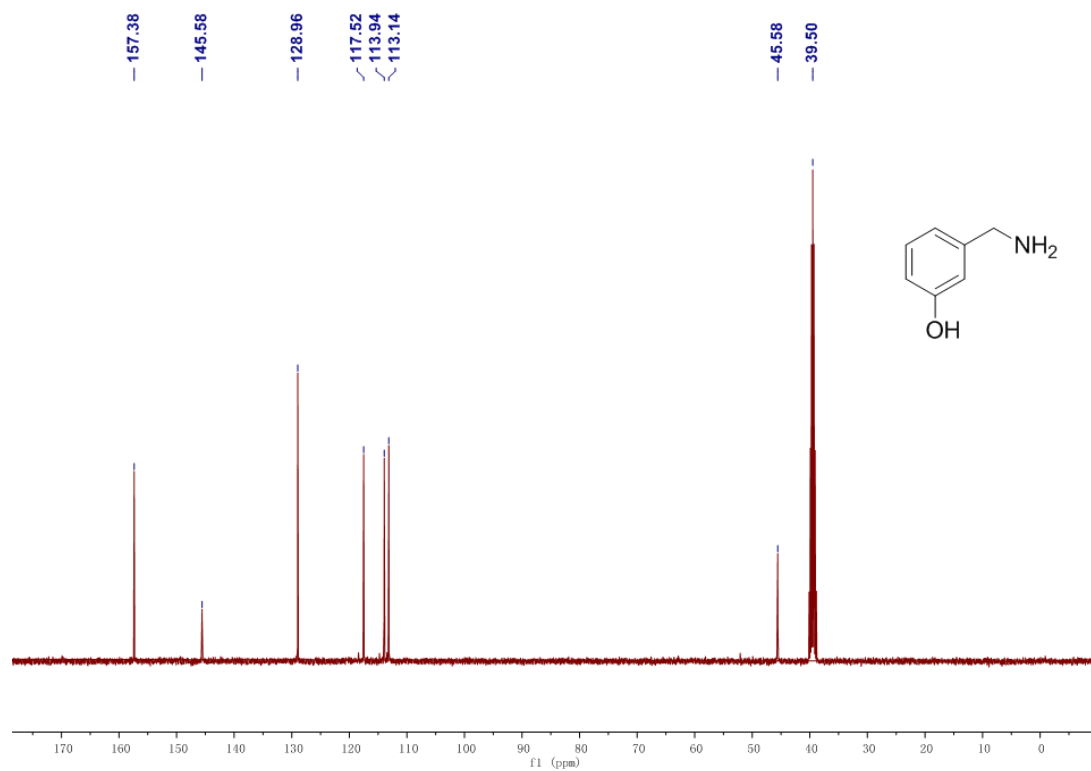


Figure S71. ¹³C NMR spectrum of isolated **3r**.

6. Standard Curves

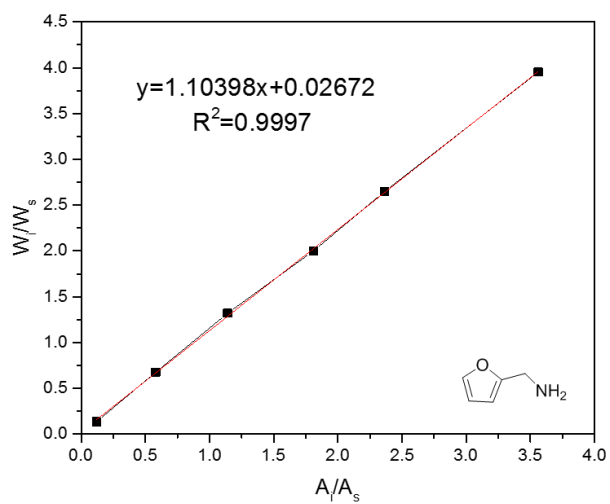


Figure S72. The standard curve of furfurylamine (**3a**).

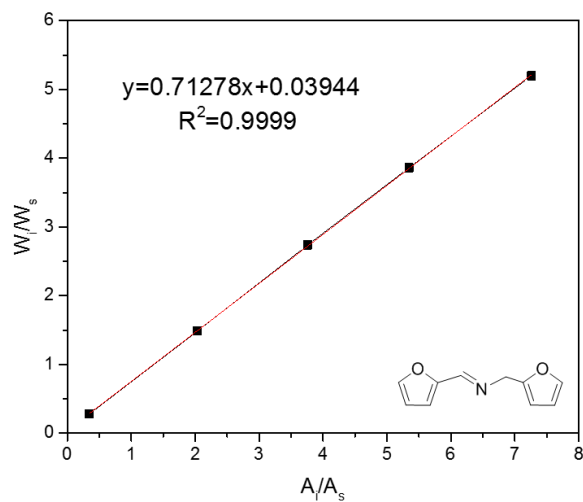


Figure S73. The standard curve of N-furfurylidene-furfurylamine (**4a**).

References

1. T. Komanoya, T. Kinemura, Y. Kita, K. Kamata and M. Hara, *J. Am. Chem. Soc.*, 2017, **139**, 11493-11499.
2. D. Deng, Y. Kita, K. Kamata and M. Hara, *ACS Sustain. Chem. Eng.*, 2019, **7**, 4692-4698.
3. W. Guo, T. Tong, X. Liu, Y. Guo and Y. Wang, *ChemCatChem*, 2019, **11**, 4130-4138.
4. D. Chandra, Y. Inoue, M. Sasase, M. Kitano, A. Bhaumik, K. Kamata, H. Hosono and M. Hara, *Chem. Sci.*, 2018, **9**, 5949-5956.
5. S. Nishimura, K. Mizuhori and K. Ebitani, *Res. Chem. Intermed.*, 2016, **42**, 19-30.
6. M. Chatterjee, T. Ishizaka and H. Kawanami, *Green Chem.*, 2016, **18**, 487-496.
7. Z. Yuan, B. Liu, P. Zhou, Z. Zhang and Q. Chi, *J. Catal.*, 2019, **370**, 347-356.
8. H. Yuan, J.-P. Li, F. Su, Z. Yan, B. T. Kusema, S. Streiff, Y. Huang, M. Pera-Titus and F. Shi, *ACS Omega*, 2019, **4**, 2510-2516.
9. N. S. Gould, H. Landfield, B. Dinkelacker, C. Brady, X. Yang and B. Xu, *ChemCatChem*, 2020, **12**, 2106-2115.
10. J. Liu, Y. Zhu, C. Wang, T. Singh, N. Wang, Q. Liu, Z. Cui and L. Ma, *Green Chem.*, 2020, **22**, 7387-7397.